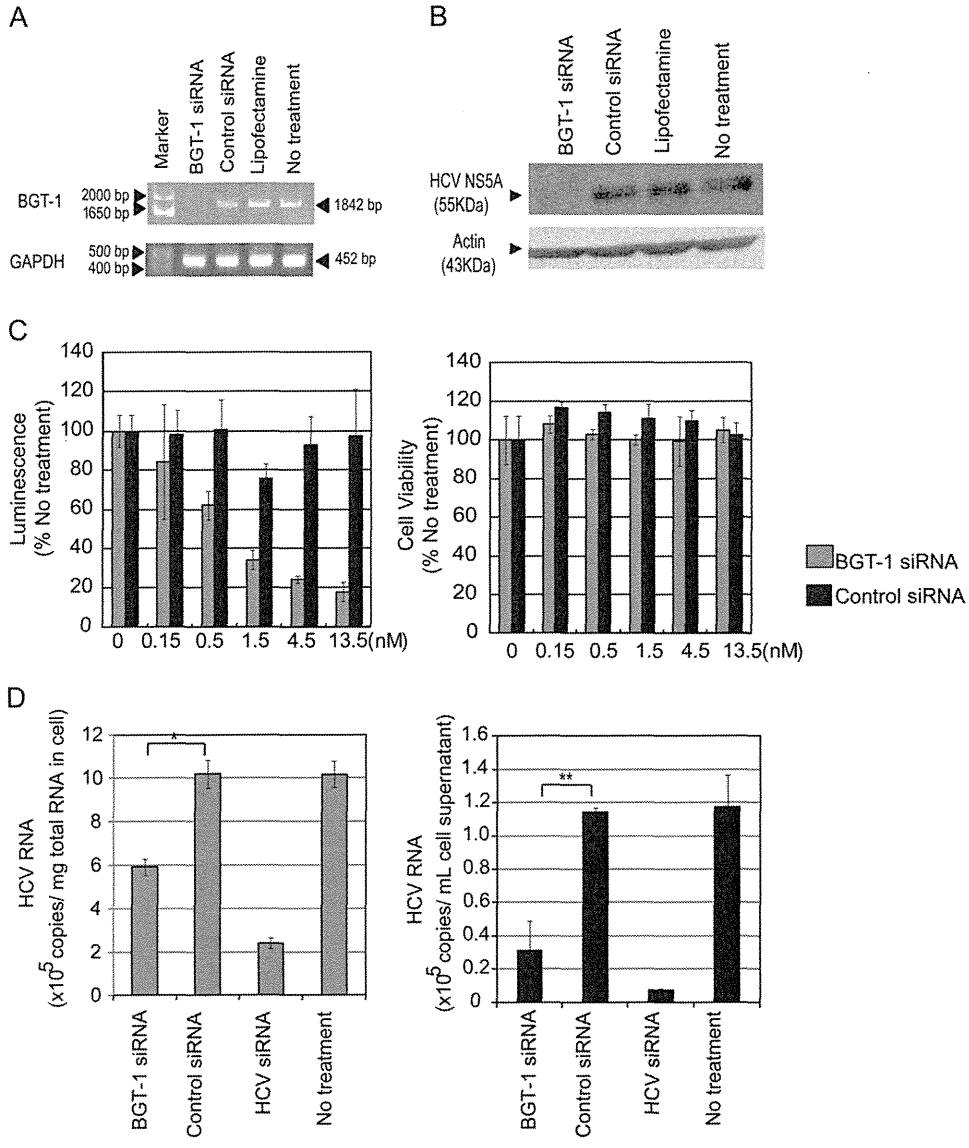

Figure 3. BGT-1 silencing by siRNA inhibits HCV replication in subgenomic HCV replicon cell lines and the persistently infected cell line. *A*, The siRNA targeting BGT-1 suppressed the expression of the corresponding mRNA. The mRNA of each sample was extracted 72 hours after siRNA (10 nM) transfection. Total RNA was transcribed and amplified by RT-PCR using primers specific to the open reading frame (ORF) of the BGT-1 (1842 bp) gene. The experiments were performed in triplicate, and the representative data are presented. *B*, The effects of BGT-1 siRNA (10 nM) on HCV were confirmed by Western blot analysis using an antibody against the HCV NS5A protein (55 kDa). The blots were striped and reprobed with an antibody directed against actin to examine protein loading in each lane. *C*, Levels of HCV replication (left panel) and cell viability (right panel) are presented according to serial concentrations of siRNA targeting BGT-1 and control siRNA in FLR3-1 cells (72 hours after transfection). The inhibition of replication or cell viability following siRNA targeting BGT-1 is defined relative to those of the cells that received no treatment (100%). The error bars represent the standard error of triplicate experiments. *D*, Quantification of HCV RNA by RTD-PCR in HCV persistently infected cells (JFH/K4) after treatment with BGT-1 siRNA. The cells were treated with siRNAs (10 nM) against BGT-1, control, and HCV (HCV R7) and harvested at 72 hours after transfection. TaqMan quantitative RT-PCR was performed for quantitation of HCV RNA in extracted RNA from cells (left panel) and their supernatants (right panel). The single asterisk (*) and double asterisk (**) indicate $P < .005$ and $P < .05$ against the control, respectively. The mean values from triplicate wells are indicated, and the vertical bars indicate the standard deviation.

those in FLR3-1 cells. The median inhibitory concentration (IC_{50}) values of BGT-1 siRNAs in various HCV replicon cell lines were as follows: FLR3-1 cells, 0.93 nM; R6FLR-N cells, 1.37 nM; JFH-1 cells, 5.95 nM. The cell viability was not significantly influenced by the siRNA treatment (Figure 3*C*, right panel; Supplementary Figure 2*A*, right panel).

Further, we monitored the levels of HCV RNA in JFH/K4 cells and their supernatants after BGT-1 silencing. Using RTD-PCR, we detected significant suppression in the HCV RNA levels by BGT-1 silencing in these cells ($P < .005$; Figure 3*D*, left panel) and their supernatants ($P < .05$; Figure 3*D*, right panel). These results were consistent with the strong inhibitory effects of

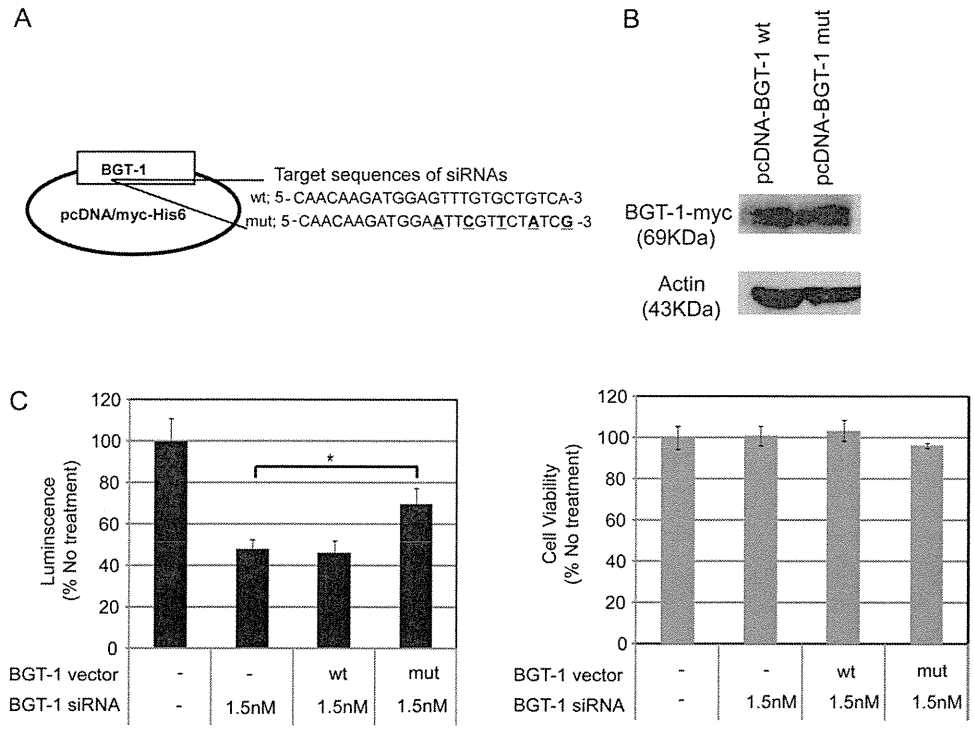

Figure 4. Validation of the inhibitory effects of BGT-1 siRNA on HCV replication in subgenomic HCV replicon cell lines. *A*, Schematic representation of the pcDNA-BGT-1 wild-type (wt) and mutant (mut) plasmids. The siRNA-targeted sites are indicated, and the underlined bold letters indicate the sequences induced by mutagenesis PCR. *B*, The wild type and mutant of the BGT-1-myc fusion protein were detected by using an anti-myc monoclonal antibody (9E10) in transfected R6FLR-N cells (upper panel). The blots were striped and reprobed with an antibody against actin to determine protein loading for each lane (lower panel). *C*, R6FLR-N cells were transfected with BGT-1 siRNA, and wild-type or mutant expression vectors were transfected after siRNA transfection. After 24 hours of vector transfection, the level of HCV replication (left panel) was measured by luminescence, and cell viability (right panel) was measured by WST-8 assay. The asterisk indicates $P < .05$ compared with transfection of siRNA alone. The mean values from triplicate wells are indicated, and the vertical bars represent the standard deviation.

BGT-1 siRNA on HCV replication, as shown in Figure 3*C*. We designed alternative siRNA targeting BGT-1 (BGT-1-siRNA-362) and observed its significant inhibitory effect on HCV replication without significant cytotoxicity (Supplementary Figure 2*B*).

Validation of the Anti-HCV Effects of siRNA Against BGT-1 by Rescue With Expression Vectors

To assess the specificity of BGT-1 silencing, we attempted to rescue HCV replication against the ectopic effects by this silencing. To examine the effect of the rescue, we constructed expression vectors of wild-type and mutant BGT-1 (Figure 4*A*) and confirmed the expression of each BGT-1-myc-fused protein (Figure 4*B*). The mutant BGT-1 vector contained 5 base mismatches within the site targeted by the BGT-1 siRNA without a change in the amino acid sequence of the protein (underlined in Figure 4*A*). We also transfected the pcDNA-BGT-1 plasmid after the siRNA treatment and observed significant recovery of HCV replication with mutant pcDNA-BGT-1 ($P < .05$; Figure 4*C*, left panel) without significant cytotoxicity (Figure 4*C*, right panel). BGT-1 expression was increased significantly in K4 cells in the presence of HCV ($P < .05$, Supplementary Figure 2*C*) at 72 hours after infection compared with the absence of HCV, and in RzM6-LC cells, which persistently express HCV [8], compared with RzM6-0d cells, which lack HCV expression ($P < .05$, Supplementary Figure 2*D*).

DISCUSSION

In this study, we determined that 2-152a MAb, which binds to but does not affect the activity of DHCR24, suppresses HCV replication and that BGT-1 is highly downregulated in HCV replicon cell lines treated with this antibody. Further, the efficient rescue of viral replication with a mutant expression vector indicates the specific inhibitory effect of BGT-1 silencing on HCV replication. Therefore, we hypothesize that BGT-1 plays an important role in HCV replication through a pathway that is likely independent of DHCR24, which in its own right can regulate the HCV life cycle [13].

BGT-1 is involved in sodium- and chloride-coupled betaine uptake, which helps in maintaining normal cellular conditions. Previous reports have described that the transcription of BGT-1 mRNA is regulated by a tonicity sensitive element (TonE) in response to hypertonic stress, a result that was first identified in the Madin-Darby canine kidney (MDCK) cell line [24]. BGT-1

is also thought to be responsible for the hyperosmotic stress response and in maintaining cell hydration. Denkert et al [25] reported that BGT-1 gene expression is induced by hyperosmolarity and inhibited by p38 mitogen-activated protein kinase ($p38^{MAPK}$) inhibitor SB20358. Further, several reports have evidenced that cell hydration affects viral replication and that viral replication increases during cell shrinkage due to hyperosmolarity, a result that was accompanied by increased BGT-1 mRNA expression [26]. Considering the reduction in HCV replication by the BGT-1 siRNA treatment, this treatment may prevent HCV replication by affecting hypoosmotic conditions in HCV-infected cells. Further studies are required to examine in detail the function of BGT-1 in HCV replication.

In summary, we demonstrated that the 2-152a monoclonal antibody inhibits HCV replication in HCV replicon cells and HCV infection in human hepatocytes transplanted into chimeric mice. The inhibitory effect of the monoclonal antibody on viral replication may be mediated by the suppression of BGT-1 expression. We propose BGT-1 as a key target for anti-HCV therapies.

Supplementary Data

Supplementary materials are available at *The Journal of Infectious Diseases* online (Supplementary Data).

Supplementary materials consist of data provided by the author that are published to benefit the reader. The posted materials are not copyedited. The contents of all supplementary data are the sole responsibility of the authors. Questions or messages regarding errors should be addressed to the author.

Notes

Acknowledgments. The authors thank I. Maruyama, K. Tanaka, T. Seki, and R. Takehara for their excellent technical support, and Y. Tokunaga for the insightful comments and helpful discussion.

Financial Support. This work was supported by grants from the Ministry of Health and Welfare of Japan; Ministry of Education, Culture, Sports, Science and Technology of Japan; Program for Promotion of Fundamental Studies in Health Sciences of the National Institute of Biomedical Innovation; and Cooperative Research Project on Clinical and Epidemiological Studies of Emerging and Reemerging Infectious Diseases.

Potential conflicts of interest. All authors: No reported conflicts.

All authors have submitted the ICMJE Form for Disclosure of Potential Conflicts of Interest. Conflicts that the editors consider relevant to the content of the manuscript have been disclosed.

References

1. Di Bisceglie AM, Carithers RL Jr, Gores GJ. Hepatocellular carcinoma. Hepatology **1998**; 28:1161–5.
2. Hayashi J, Aoki H, Arakawa Y, Hino O. Hepatitis C virus and hepatocarcinogenesis. Intervirology **1999**; 42:205–10.
3. Michielsen PP, Francque SM, van Dongen JL. Viral hepatitis and hepatocellular carcinoma. World J Surg Oncol **2005**; 3:27.
4. Mazzella G, Accogli E, Sottili S, et al. Alpha interferon treatment may prevent hepatocellular carcinoma in HCV-related liver cirrhosis. J Hepatol **1996**; 24:141–7.
5. Bruchfeld A, Stahle L, Andersson J, Schvarcz R. Ribavirin treatment in dialysis patients with chronic hepatitis C virus infection—a pilot study. J Viral Hepat **2001**; 8:287–92.
6. Kohara M, Tanaka T, Tsukiyama-Kohara K, et al. Hepatitis C virus genotypes 1 and 2 respond to interferon-alpha with different virologic kinetics. J Infect Dis **1995**; 172:934–8.
7. Nakamura H, Ogawa H, Kuroda T, et al. Interferon treatment for patients with chronic hepatitis C infected with high viral load of genotype 2 virus. Hepatogastroenterology **2002**; 49:1373–6.
8. Tsukiyama-Kohara K, Toné S, Maruyama I, et al. Activation of the CKI-CDK-Rb-E2F pathway in full genome hepatitis C virus-expressing cells. J Biol Chem **2004**; 279:14531–41.
9. Crameri A, Biondi E, Kuehnle K, et al. The role of seladin-1/DHCR24 in cholesterol biosynthesis, APP processing and Aβ generation in vivo. EMBO J **2006**; 25:432–43.
10. Waterham HR, Koster J, Romeijn GJ, et al. Mutations in the 3β-hydroxysterol Δ^{24}-reductase gene cause desmosterolosis, an autosomal recessive disorder of cholesterol biosynthesis. Am J Hum Genet **2001**; 69:685–94.
11. Lu X, Kambe F, Cao X, et al. 3β-Hydroxysteroid-Δ24 reductase is a hydrogen peroxide scavenger, protecting cells from oxidative stress-induced apoptosis. Endocrinology **2008**; 149:3267–73.
12. Nishimura T, Kohara M, Izumi K, et al. Hepatitis C virus impairs p53 via persistent overexpression of 3β-hydroxysterol Δ24-reductase. J Biol Chem **2009**; 284:36442–52.
13. Takano T, Tsukiyama-Kohara K, Hayashi M, et al. Augmentation of DHCR24 expression by hepatitis C virus infection facilitates viral replication in hepatocytes. J Hepatol **2011**; 55:512–21.
14. Lohmann V, Körner F, Koch J, Herian U, Theilmann L, Bartenschlager R. Replication of subgenomic hepatitis C virus RNAs in a hepatoma cell line. Science **1999**; 285:110–3.
15. Watanabe T, Sudoh M, Miyagishi M, et al. Intracellular-diced dsRNA has enhanced efficacy for silencing HCV RNA and overcomes variation in the viral genotype. Gene Ther **2006**; 13:883–92.
16. Sakamoto H, Okamoto K, Aoki M, et al. Host sphingolipid biosynthesis as a target for hepatitis C virus therapy. Nat Chem Biol **2005**; 1:333–7.
17. Kato T, Date T, Miyamoto M, et al. Efficient replication of the genotype 2a hepatitis C virus subgenomic replicon. Gastroenterology **2003**; 125: 1808–17.
18. Blight KJ, McKeating JA, Rice CM. Highly permissive cell lines for subgenomic and genomic hepatitis C virus RNA replication. J Virol **2002**; 76:13001–14.
19. Wakita T, Pietschmann T, Kato T, et al. Production of infectious hepatitis C virus in tissue culture from a cloned viral genome. Nat Med **2005**; 11:791–6.
20. Mercer DF, Schiller DE, Elliott JF, et al. Hepatitis C virus replication in mice with chimeric human livers. Nat Med **2001**; 7:927–33.
21. Inoue K, Umehara T, Ruegg UT, et al. Evaluation of a cyclophilin inhibitor in hepatitis C virus-infected chimeric mice in vivo. Hepatology **2007**; 45:921–8.
22. Takeuchi T, Katsume A, Tanaka T, et al. Real-time detection system for quantification of hepatitis C virus genome. Gastroenterology **1999**; 116:636–42.
23. Sarkar D, Imai T, Kambe F, et al. The human homolog of Diminuto/Dwarf1 gene (hDiminuto): a novel ACTH-responsive gene overexpressed in benign cortisol-producing adrenocortical adenomas. J Clin Endocrinol Metab **2001**; 86:5130–7.
24. Takenaka M, Preston AS, Kwon HM, Handler JS. The tonicity-sensitive element that mediates increased transcription of the betaine transporter gene in response to hypertonic stress. J Biol Chem **1994**; 269: 29379–81.
25. Denkert C, Warskulat U, Hensel F, Häussinger D. Osmolyte strategy in human monocytes and macrophages: involvement of p38MAPK in hyperosmotic induction of betaine and myoinositol transporters. Arch Biochem Biophys **1998**; 354:172–80.
26. Häussinger D. The role of cellular hydration in the regulation of cell function. Biochem J **1996**; 313:697–710.

JOURNAL OF VIROLOGY, Jan. 2010, p. 303–311 Vol. 84, No. 1
0022-538X/10/$12.00 doi:10.1128/JVI.01448-09

Pathogenesis of Hepatitis C Virus Infection in *Tupaia belangeri*▽†

Yutaka Amako,[1] Kyoko Tsukiyama-Kohara,[1,2] Asao Katsume,[1,3] Yuichi Hirata,[1] Satoshi Sekiguchi,[1] Yoshimi Tobita,[1] Yukiko Hayashi,[4] Tsunekazu Hishima,[4] Nobuaki Funata,[4] Hiromichi Yonekawa,[5] and Michinori Kohara[1]*

Department of Microbiology and Cell Biology, Tokyo Metropolitan Institute of Medical Science, 2-1-6, Kamikitazawa, Setagaya-ku, Tokyo 156-0057, Japan[1]; Department of Experimental Phylaxiology, Faculty of Medical and Pharmaceutical Sciences, Kumamoto University, 1-1-1 Honjo Kumamoto City, Kumamoto 860-8556, Japan[2]; Fuji Gotemba Research Laboratory, Chugai Pharmaceutical Company, Ltd., 135, Komakado 1 Chome, Gotemba-shi, Shizuoka 412-8513, Japan[3]; Department of Pathology, Tokyo Metropolitan Komagome Hospital, 3-18-22 Honkomagome, Bunkyo-ku, Tokyo 113-8677, Japan[4]; and Laboratory of Animal Science, Tokyo Metropolitan Institute of Medical Science, 2-1-6, Kamikitazawa, Setagaya-ku, Tokyo 156-0057, Japan[5]

Received 14 July 2009/Accepted 5 October 2009

The lack of a small-animal model has hampered the analysis of hepatitis C virus (HCV) pathogenesis. The tupaia (*Tupaia belangeri*), a tree shrew, has shown susceptibility to HCV infection and has been considered a possible candidate for a small experimental model of HCV infection. However, a longitudinal analysis of HCV-infected tupaias has yet to be described. Here, we provide an analysis of HCV pathogenesis during the course of infection in tupaias over a 3-year period. The animals were inoculated with hepatitis C patient serum HCR6 or viral particles reconstituted from full-length cDNA. In either case, inoculation caused mild hepatitis and intermittent viremia during the acute phase of infection. Histological analysis of infected livers revealed that HCV caused chronic hepatitis that worsened in a time-dependent manner. Liver steatosis, cirrhotic nodules, and accompanying tumorigenesis were also detected. To examine whether infectious virus particles were produced in tupaia livers, naive animals were inoculated with sera from HCV-infected tupaias, which had been confirmed positive for HCV RNA. As a result, the recipient animals also displayed mild hepatitis and intermittent viremia. Quasispecies were also observed in the NS5A region, signaling phylogenic lineage from the original inoculating sequence. Taken together, these data suggest that the tupaia is a practical animal model for experimental studies of HCV infection.

Hepatitis C virus (HCV) is a small enveloped virus that causes chronic hepatitis worldwide (32). HCV belongs to the genus *Hepacivirus* of the family *Flaviviridae*. Its genome comprises 9.6 kb of single-stranded RNA of positive polarity flanked by highly conserved untranslated regions at both the 5′ and 3′ ends (4, 27, 29). The 5′ untranslated region harbors an internal ribosomal entry site (29) that initiates translation of a single open reading frame encoding a large polyprotein comprising about 3,010 amino acids (35). The encoded polyprotein is co- and posttranslationally processed into 10 individual viral proteins (15).

In most cases of human infection, HCV is highly potent and establishes lifelong persistent infection, which progressively leads to chronic hepatitis, liver steatosis, cirrhosis, and hepatocellular carcinoma (9, 16, 21). The most effective therapy for treatment of HCV infection is administration of pegylated interferon combined with ribavirin. However, the combination therapy is an arduous regimen for patients; furthermore, HCV genotype 1b does not respond efficiently (19). The prevailing scientific opinion is that a more viable option than interferon treatment is needed.

The chimpanzee is the only validated animal model for in vivo studies of HCV infection, and it is capable of reproducing most aspects of human infection (5, 18, 23, 28, 35, 36). The chimpanzee is also the only validated animal for testing the authenticity and infectivity of cloned viral sequences (8, 14, 35, 36). However, chimpanzees are relatively rare and expensive experimental subjects. Cross-species transmission from infected chimpanzees to other nonhuman primates has been tested but has proven unsuccessful for all species evaluated (1).

The tupaia (*Tupaia belangeri*), a tree shrew, is a small nonprimate mammal indigenous to certain areas of Southeast Asia (6). It is susceptible to infection with a wide range of human-pathogenic viruses, including hepatitis B viruses (13, 20, 31), and appears to be permissive for HCV infection (33, 34). In an initial report, approximately one-third of inoculated animals exhibited acute, transient infection, although none developed the high-titer sustained viremia characteristic of infection in humans and chimpanzees (33). The short duration of follow-up precluded any observation of liver pathology. In addition to the putative in vivo model, cultured primary hepatocytes from tupaias can be infected with HCV, leading to de novo synthesis of HCV RNA (37). These reports strongly support tupaias as a valid model for experimental studies of HCV infection. However, longitudinal analyses evaluating the clinical development and pathology of HCV-infected tupaias have yet to be exam-

* Corresponding author. Mailing address: Department of Microbiology and Cell Biology, The Tokyo Metropolitan Institute of Medical Science, 2-1-6, Kamikitazawa, Setagaya-ku, Tokyo 156-0057, Japan. Phone: 81-3-5316-3232. Fax: 81-3-5316-3137. E-mail: kohara-mc@igakuken.or.jp.

† Supplemental material for this article may be found at http://jvi.asm.org/.

▽ Published ahead of print on 21 October 2009.

TABLE 1. Experimental HCV infections performed in this study

Tupaia no.	Inoculum		Biopsy/sacrifice[b]
	Type	Quantity (GE/tupaia)[a]	
Group I[c]			
Tup.4	RCV	1×10^7	84, 94/144 wk p.i.
Tup.5	HCR6	6×10^5	95, 105/155 wk p.i.
Tup.6	HCR6	6×10^5	95, 105/155 wk p.i.
Tup.8	RCV	1×10^7	84, 94/144 wk p.i.
Group II[d]			
Tup.9	Tup.5 (5 wk p.i.)	1×10^2	NT
Tup.10	Tup.5 (5 wk p.i.)	1×10^2	NT
Tup.11	Tup.8 (10 wk p.i.)	1×10^2	NT
Tup.12	Tup.8 (10 wk p.i.)	1×10^2	NT
Tup.13	Tup.4 (8 wk p.i.)	1×10^2	NT
Tup.14	Tup.4 (8 wk p.i.)	1×10^2	NT
Group III[e]			
Tup.15	None		92/100 wk
Tup.17	None		92/100 wk
Tup.38	None		242 wk
Tup.39	None		242 wk

[a] Viral RNA GE/tupaia was estimated by Quantitative real-time RT-PCR (GE, genome equivalents; sensitivity > 10 GE/ml serum).
[b] Liver biopsy was performed at indicated time-point. p.i., postinoculation; NT, not tested.
[c] Group I, primary infection experiment in which 1-year-old animals were inoculated with two different types of inocula.
[d] Group II, reinfection experiment, where HCV RNA-positive sera from Group I experimental infections were passaged to naive animals.
[e] GroupIII, no-infection control.

ined. In the present study, we describe the clinical development and pathology of HCV-infected tupaias over an approximately 3-year time course.

MATERIALS AND METHODS

Animals. Table 1 summarizes the tupaias used in this study. Tupaias born in laboratory captivity were obtained from the Laboratory Animal Center at the Kunming Institute of Zoology (Chinese Academy of Sciences). Tupaias were imported with permission from the Convention on International Trade in Endangered Species of Wild Fauna and Flora (7), quarantined for medical inspection, and housed individually in standard rat cages supplied with filtered air. The animals were fed a daily regimen of eggs, fruit, and the CMS-1 commercial diet for marmosets (CLEA, Japan). Their appetites and feces were carefully monitored. Animal care and experimental handling conformed to study guidelines established by the Subcommittee on Laboratory Animal Care at the Tokyo Metropolitan Institute of Science.

Patient serum used for animal infection. HCV genotype 1b serum, designated HCR6, was obtained from a patient with chronic active hepatitis C. The infectious titer of HCR6 was determined in chimpanzee and Molt4 cells and denoted plasma K (HCR6) by Shimizu et al. (24). The HCR6 serum exhibited a PCR titer of 6×10^6 genome equivalents/ml and an infectious titer of 3.7×10^4 50% chimpanzee infectious doses/ml. Serum aliquots were frozen at −80°C until they were used.

Virion reconstitution of cloned HCV. As described previously, pHCR6 (genotype 1b; 9,611 nucleotides; GenBank accession no. AY045720) is a plasmid carrying HCV genomic cDNA cloned from HCR6 serum (30). pHCR6Rz was designed for precisely trimmed RNA expression, with the entire genomic region of pHCR6Rz recloned under the control of the T7 promoter and the 5′ and 3′ distal ends flanked by hammerhead- and hepatitis D virus ribozyme-encoding sequences, respectively (22, 25).

For molecular reconstitution of HCV particles, pHCR6Rz was transfected into IMY-N9 cells as described previously (12). Briefly, semiconfluent IMY-N9 cells in 100-mm plastic dishes were transfected with 15 μg of plasmid using 40 μl of cationic lipids (DMRIE-C reagent; Life Technology) in accordance with the manufacturer's instructions. Five hours after transfection, the cells were infected with AdexCAT7 (2) (kindly provided by Y. Matsuura) at a multiplicity of infection of 20. After infection, the culture medium was replaced with Hepato-STIM (Becton Dickinson). The culture supernatants were collected at 24 h postinfection and stored at −80°C.

Virus inoculation and collection of serum samples. Animals were infected at 6 months of age. The anesthetic agent, ketamine hydrochloride, was administered intramuscularly at 50 mg/kg body weight prior to virus inoculation and bleeding of the tupaias. The inocula were introduced intravenously at 6×10^5 genome equivalents/animal for patient serum HCR6 and 1×10^7 genome equivalents/animal for reconstituted virions derived from the pHCR6Rz inoculation. Blood samples were drawn from infected and control animals pre- and postinfection. Briefly, the animals were bled weekly for 20 weeks and biweekly thereafter. At each time point, 0.5 ml of blood was drawn from the thigh vein; the sera were separated, aliquoted, and stored for subsequent assays.

Reinfection experiments were performed by transmission of HCV RNA-positive serum from group I (Table 1) to naive animals.

Serum alanine aminotransferase (ALT) concentrations were determined using a Transnase Nissui kit (Nissui Pharmaceutical Co.), standardized, and displayed as IU/liter.

RNA isolation and quantitative RTD-PCR assay for HCV RNA. Serum samples (100 μl) were tested for circulating HCV RNA in vivo using quantitative real-time detection (RTD)-PCR (TaqMan). RNA was extracted from the sera and livers of sacrificed animals using the acid guanidium-phenol chloroform method with tRNA as a carrier (3). Two tupaias (Tup.5 and Tup.6) were inoculated with patient serum HCR6. Another two animals (Tup.4 and Tup.8) were inoculated with reconstituted viral particles (RCV). Tup.15 served as a mock-infected control. Liver specimens (3- to 4-mm^2 blocks) from these tupaias were homogenized with 1.5 ml of 5 M guanidine thiocyanate using a polytron-type homogenizer (Ultra-Turrax T25; IKA Laborteehnik, Staufen, Germany). RNA was then reextracted with 4 M guanidine thiocyanate.

RNA samples were subjected to RTD-PCR on an ABI 7700 sequence detector (Applied Biosystems) as described previously (26). The extracted RNA was dissolved in 200 μl of diethyl pyrocarbonate-treated water containing 10 mM dithiothreitol and 200 units/ml RNase inhibitor in a siliconized tube. RTD-PCR was performed using 1 μg of total RNA, one set of PCR primers, and a probe for a location within the 5′ noncoding region using the EZ r*Tth* RNA PCR kit (Perkin Elmer) and the ABI Prism 7700 sequence detector system. A standard curve was constructed using a 10-fold dilution series of in vitro-transcribed and previously titrated synthetic HCV RNA.

Consequently, the quantities represented by genome equivalents correspond to an absolute standard curve (26). All quantitative RTD-PCR assays were performed using duplicate samples, with both negative control serum and HCV-positive serum included. The control sera were diluted before use and were estimated to contain low copy numbers of HCV RNA (100 genome equivalents/ml serum). Samples were deemed positive for HCV RNA if both duplicates yielded PCR-amplified product. Averages of the two estimated values are shown in the figures.

Histological analysis. Tissue samples were carefully collected from anesthetized animals by abdominal incision, fixed in 10% neutral buffered formalin, embedded in paraffin, sectioned, and stained with hematoxylin and eosin (H&E). Silver and Sudan IV (Wako Pure Chemical Industries, Ltd.) staining were also carried out to visualize fiber generation and lipid degeneration, respectively. All histological staining was performed in accordance with conventional procedures. The histological status was determined using the modified hepatitis activity index scoring system, which grades necrosis and inflammation on a scale of 0 to 18 (periportal inflammation and necrosis, 0 to 10; lobular inflammation and necrosis, 0 to 4; portal inflammation, 0 to 4) (11). Fibrosis was scored using the Ishak fibrosis scale of 0 to 6 (0, no fibrosis; 1 or 2, portal fibrosis; 3 or 4, bridging fibrosis; and 5 or 6, cirrhosis). The values in each group (Table 2) represent the averages of the scores in five visual fields.

Statistical analysis. The statistical significance of differences between controls and HCV-infected animals was analyzed with the nonparametric Mann-Whitney U test. All comparisons were two tailed. The statistical analysis was conducted with SPSS 12.0 software (SPSS Inc., Chicago, IL).

RESULTS

Inoculation of HCV causes acute hepatitis and transient viremia in tupaias. To begin this study, two distinct but related inocula were chosen for infection of tupaias. Serum from a chronic hepatitis patient (designated HCR6) was chosen for its

TABLE 2. Grading: necroinflammatory scores and fibrosis

Group	Inoculum	Tupaia no.	Grade				Total	Avg	SD	Staging
			A	B	C	D				
94 wk p.i. (biopsy)										
I	HCR 6	Tup.5	0	0	0	0	0	1.3	1.5	0
		Tup.6	1	0	1	0	2			0
	RCV	Tup.4	0	0	0	0	0			0
		Tup.8	0	0	0	3	3			6
	Control	Tup.15	0	0	0	0	0	0	0	0
III		Tup.17	0	0	0	0	0			0
		Tup.38								
		Tup.39								
144 wk p.i. (sacrifice)										
I	HCR 6	Tup.5	1	0	2	3	6	5.5	3.7	0
		Tup.6	3	0	4	3	10			1
	RCV	Tup.4	0	0	0	1	1			0
		Tup.8	1	0	1	3	5			6
	Control	Tup.15						0	0	
III		Tup.17								
		Tup.38	0	0	0	0	0			0
		Tup.39	0	0	0	0	0			0

defined genotype (genotype 1b), and genetic heterogeneity was ascertained by the process of cloning consensus cDNA. The infectivity of this serum was also experimentally defined in chimpanzees; a 50% chimpanzee infectious dose was estimated at 3.7×10^4 50% chimpanzee infectious doses/ml. Furthermore, the consensus genomic sequence of HCV was cloned from the serum (pHCR6; 9,611 bases; GenBank AY045702.1). For the second inoculum (referred to as RCV), clonal viral particles were reconstituted as described in Materials and Methods. This inoculum was expected to be free of neutralizing antibodies and thus was considered potentially more infectious than patient sera. In the case of RCV infection, genetic diversification of viral RNA, also known as quasispecies, can be regarded as a direct indication of de novo synthesis of progenitor virus in vivo.

Either patient serum or cDNA-derived RCV was inoculated into tupaias (Table 1, group I). Two animals (one female and one male) were tested against each inoculum. Age-matched animals were bred as infection-free controls.

All experimental infections are described in Materials and Methods and Table 1. Prior to experimental infection, the normal serum ALT level in tupaias was measured at 22.3 IU/liter ($n = 23$).

Inoculation with patient serum HCR6 caused rapid fluctuations in the serum ALT concentrations, from two- to fivefold, in both inoculated tupaias, suggesting acute hepatitis in vivo (Fig. 1A and B). Correlative quantitative RTD-PCR revealed HCV viremia soon after serum inoculation in Tup.5, which continued to show transient viremia long term. The appearance of viremia sometimes coincided with a steep elevation in the serum ALT (Fig. 1A). Conversely, HCV RNA was not detected in the serum of Tup.6 up to 60 weeks postinoculation and only twice thereafter. Acute-phase ALT elevations (3 to 4 weeks postinoculation) in Tup.6 might represent tight control of HCV infection by the host immune system (Fig. 1B).

Distinct results were obtained for the two animals (Tup.4 and Tup.8) inoculated with RCV. Both animals displayed sustained viremia up to 10 weeks postinoculation (Fig. 1C and D), indicating persistent HCV infection and inability to eradicate the virus. Viremia was detected intermittently throughout the course of infection, sometimes accompanying the elevation of serum ALT. Humoral immune responses in Tup.5 and Tup.6 (see Fig. S1A in the supplemental material) and Tup.4 and Tup.6 (see Fig. S1B in the supplemental material) were indicated.

We performed RTD-PCR to confirm whether HCV could replicate in the tupaias' livers (Tup.4, Tup.5, Tup.6, and Tup.8) and obtained the following results (Fig. 1E): 310 ± 117 copies/μg total RNA in Tup.5, 80 ± 11 copies/μg in Tup.6, 199 ± 77 copies/μg in Tup.4, and 292 ± 48 copies/μg in Tup.8. In contrast, HCV RNA was not detected in the liver of the mock-infected animal (Tup.15).

HCV RNA was also not detected in samples from either preinoculation or age-matched, infection-free control tupaias (Table 1, group III), nor were significant elevations in serum ALT observed for any of the three infection-free controls (data not shown).

HCV causes chronic hepatitis in tupaia liver, leading to fibrosis and cirrhosis. Serum ALT and circulating HCV RNA levels in primary infected tupaias (Table 1, group I) were monitored for 3 years postinoculation. As described above, the magnitudes of serum ALT fluctuations varied substantially among infected animals (Fig. 1A, B, C, and D). Tupaia livers were examined for histological lesions in order to elucidate if HCV caused chronic hepatitis. Liver biopsies via abdominal incisions were performed at 2 years postinoculation. All animals were sacrificed at 3 years postinoculation (4.5 years for uninfected animals). H&E staining of liver specimens from HCV-infected tupaias showed infiltrating lymphocytes within sinusoids and around portal areas, indicating chronic hepatitis in the tupaia livers (Fig. 2B, D, and H). Infiltrating lymphocytes were also observed in limiting plates, indicating ongoing inflammation (Fig. 2G and H). Furthermore, a comparison of liver samples at 2 and 3 years postinoculation revealed that the

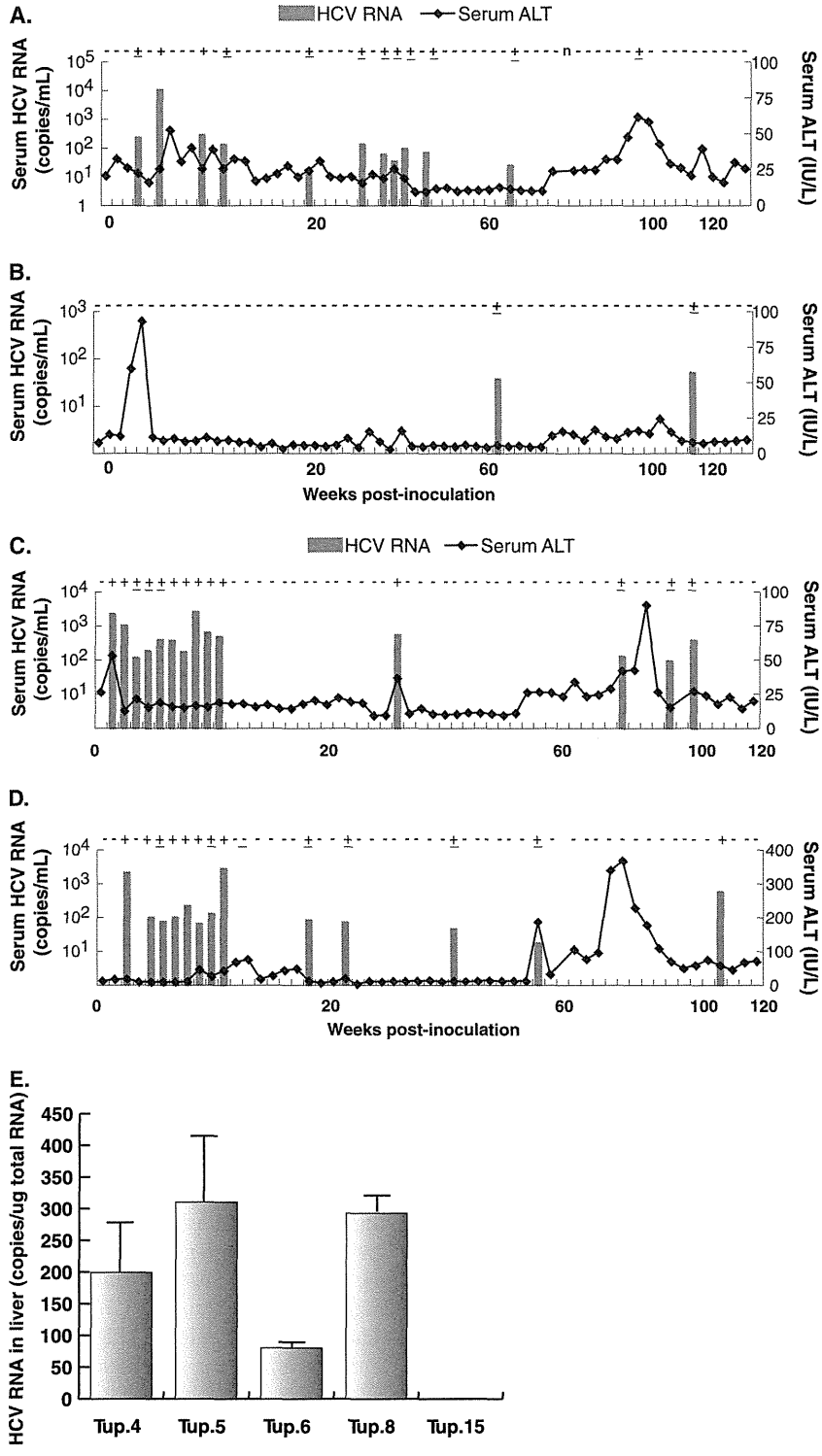

FIG. 1. Course of infection with patient serum HCR6 and RCV. (A) The results of quantitative RTD-PCR for HCV RNA and serum ALT concentrations were combined and plotted to show the course of infection in Tup.5. The bars and the ordinates on the left represent HCV RNA as genome equivalents/ml of serum. The curved line and the ordinates on the right represent serum ALT concentrations as IU/liter serum. (B) Serum HCV RNA and ALT concentrations for infection of Tup.6. (C) The graph for Tup.4. (D) The graph for Tup.8. The vertical axis for serum ALT in this graph is scaled differently from the others because of significant ALT elevation. (E) Quantification of HCV RNA in tupaia liver. HCV RNA in hepatocytes from tupaia (Tup.4, Tup.5, Tup.6, Tup.8, and Tup.15) livers was isolated 172 weeks after HCV infection and quantified by RTD-PCR. As few as 10 copies of the genome were detected, and the quantification range was between 10^1 and 10^8 copies (26).

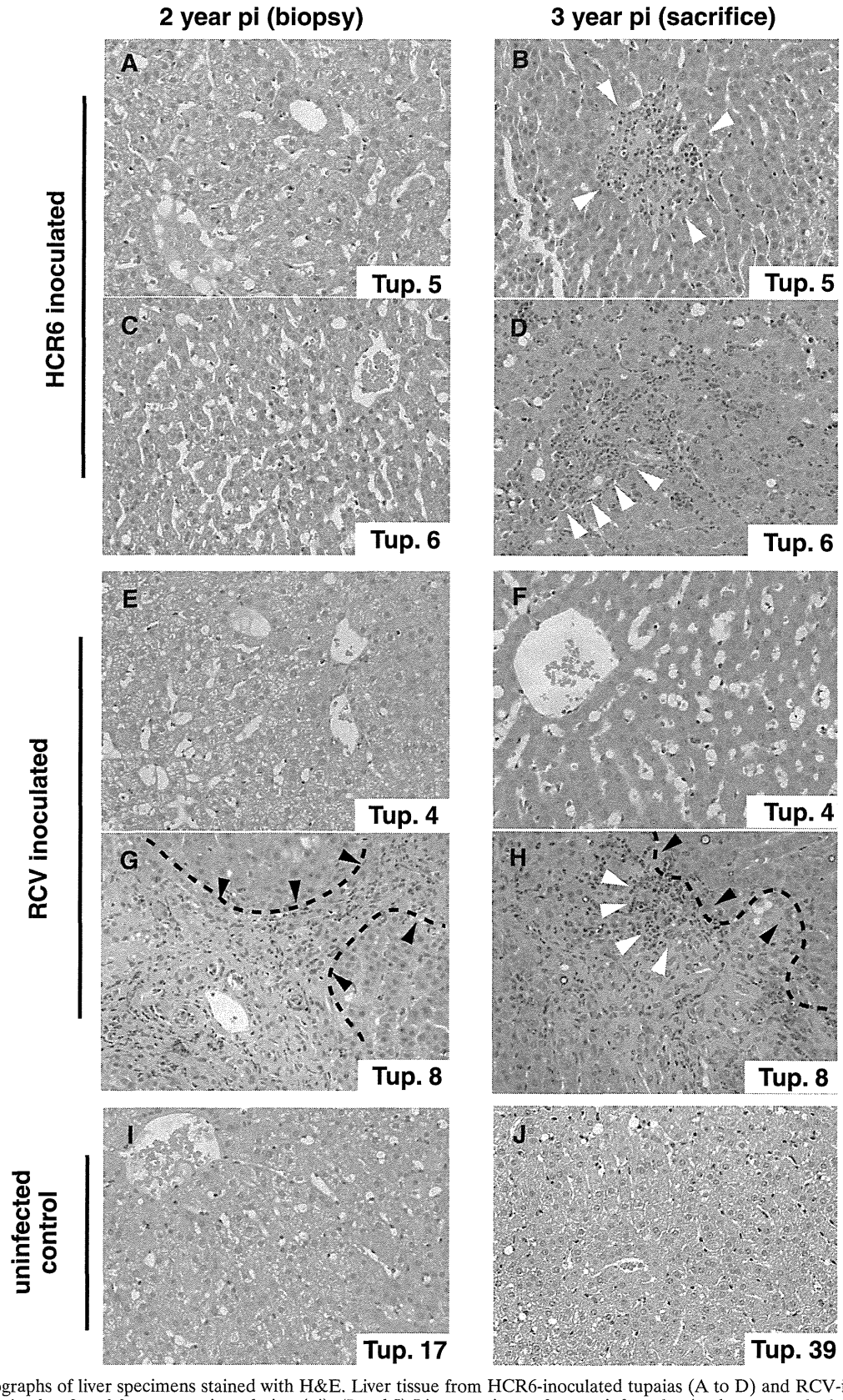

FIG. 2. Micrographs of liver specimens stained with H&E. Liver tissue from HCR6-inoculated tupaias (A to D) and RCV-inoculated tupaias (E to H) was obtained at 2 and 3 years postinoculation (pi). (I and J) Liver specimens from uninfected animals age matched to each inoculated animal were also obtained. The HCV-infected tupaia livers harbored infiltrating lymphocytes (white arrowheads) and fibrosis (broken lines and black arrowheads), which indicate chronic hepatitis.

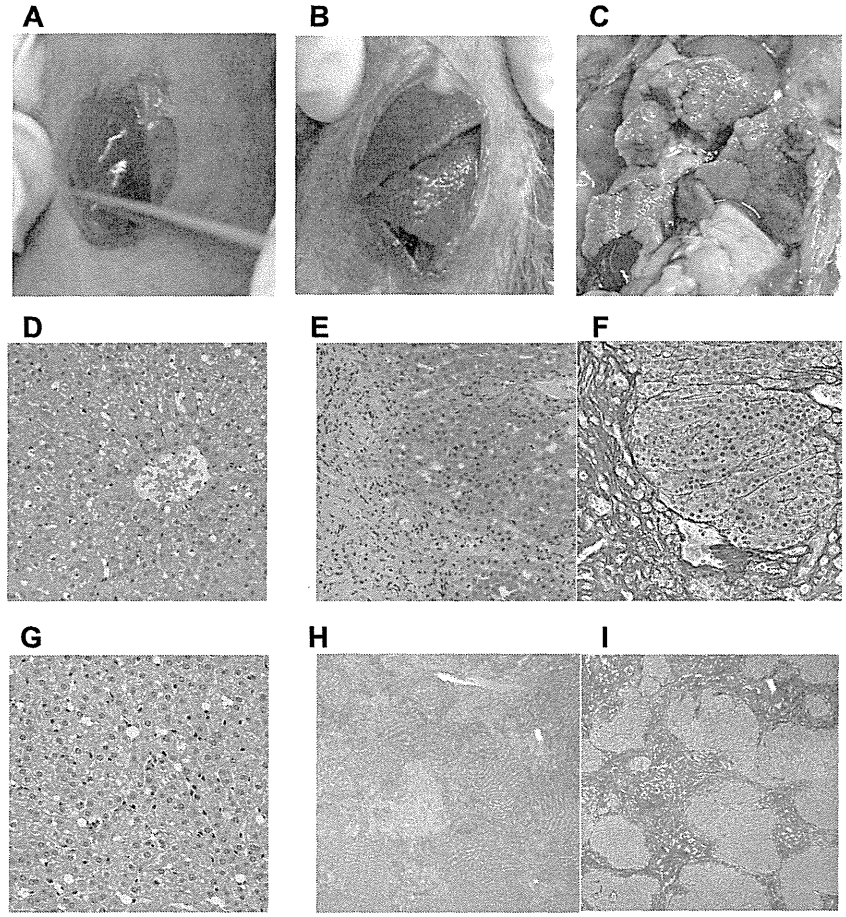

FIG. 3. Macro- and microscopic features of tupaia liver. (A) Infection-free control tupaia (Tup.15; 92 weeks). (B) RCV-infected animal displaying liver cirrhosis (Tup.8; 84 weeks postinoculation). (C) RCV-infected animal with massive surface nodules (Tup.8; 144 weeks postinoculation). (D and G) H&E staining of the uninfected Tup.15 at 92 weeks (D) and the uninfected Tup.39 at 242 weeks (G). (E, F, H, and I) H&E and silver staining of Tup.8 at 84 weeks postinoculation (E and F) or at 144 weeks postinoculation (H and I).

hepatitis had worsened with time in all HCV-infected tupaias (Fig. 2A to H and Table 2).

Fibrosis and cirrhosis were also examined. Mild fibrosis was seen in Tup.6, while severe fibrosis was seen in Tup.8. Cirrhosis was histologically investigated in all animals (Table 2). There was no significant difference between groups I and III at 94 weeks postinfection ($P = 0.194$), but at 144 weeks postinfection, a slight difference was observed ($P = 0.059$; SPSS 12.0). Macroscopic observation of the liver biopsy specimens (taken 2 years postinoculation) indicated liver cirrhosis in Tup.8 (Fig. 3B) compared with Tup.15 (uninfected control) (Fig. 3A), while silver staining of histology samples revealed fibrosis and cirrhotic nodules (Fig. 3E and F). Macroscopic observation upon sacrifice (3 years postinoculation) indicated that liver cirrhosis in Tup.8 had worsened (Fig. 3C). In contrast, age-matched infection-free negative control tupaias displayed none of these pathologies (Fig. 3A, D, and G).

Progressive lipid degeneration was noted in infected tupaias throughout the course of infection (Fig. 4). In particular, Tup.5 displayed microvesicular lipid droplets in the first biopsy specimens (at 2 years), which developed into macrovesicular droplets and foamy degeneration in biopsy specimens at 3 years (Fig. 4C and D). Liver specimens from other infected animals displayed intracellular micro- and macrovesicular lipid droplets in hepatocytes at 3 years postinoculation (Fig. 4F, H, and J). These anomalies were not present in liver specimens from infection-free control animals (Fig. 4A and B).

Transmission of viral-RNA-positive serum to naive animals reproduces acute hepatitis and viremia. To confirm virion regeneration in vivo, and to exclude the possibility of false-positive serum HCV RNA results due to amplification of the original inocula, HCV RNA-positive sera from primary inoculated tupaias were used to inoculate naive tupaias. Three different sera were tested in this passage experiment, with two naive tupaias used as recipient animals for each trial (see Materials and Methods) (Table 1, group II).

In the first reinfection experiment, serum from Tup.5 (originally infected with patient serum HCR6) was collected at 5 weeks postinoculation and used to infect two naive animals. The recipient animals showed intermittent viremia over the subsequent 3 months (Fig. 5A). In the second and third cases of reinfection, sera from Tup.8 at 10 weeks postinoculation and from Tup.4 at 8 weeks postinoculation also induced viremia in the naive inoculated animals, similar to the first reinfection experiment (Fig. 5B and C). Furthermore, the PCR titers of the recipient tupaias were significantly greater than the inoc-

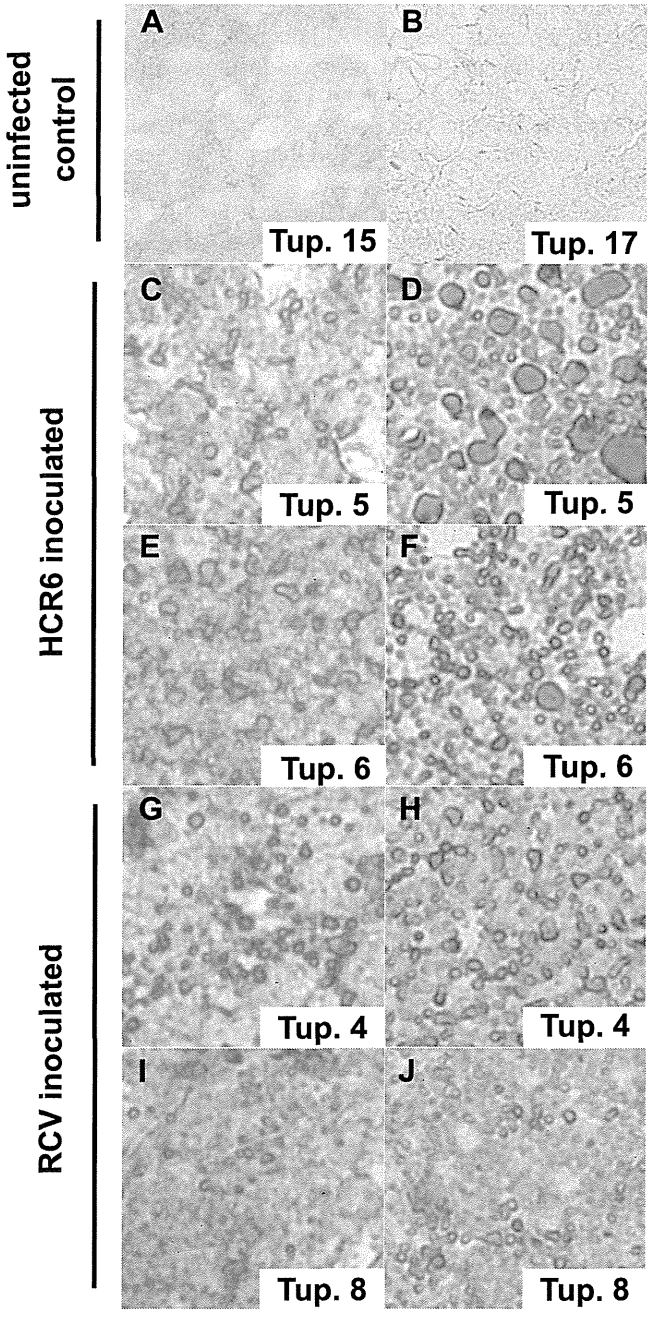

FIG. 4. Sudan IV-stained liver specimens exhibiting fatty liver degeneration. Cryosections of liver stained by Sudan IV as described in Materials and Methods show fatty liver degeneration. The left and right columns display biopsy specimens of infected animals (2 years postinoculation) and animals sacrificed at 3 years postinfection, respectively. (A and B) Uninfected controls at 2 years (Table 1 shows sample timing). (C to F) Patient serum HCR6-infected animals. (G to J) RCV-infected animals.

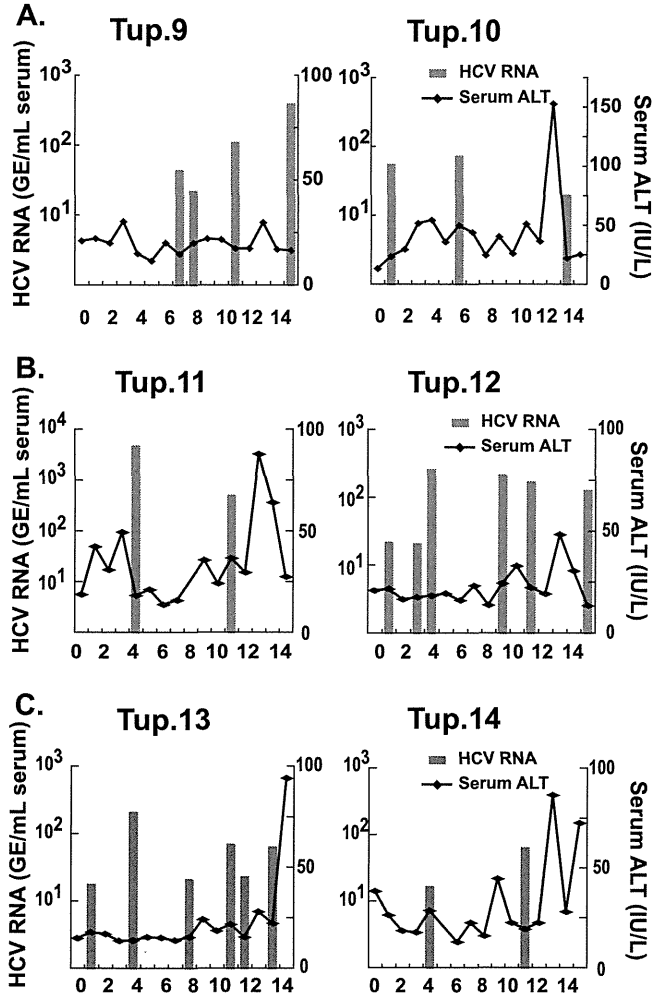

FIG. 5. Results of a reinfection experiment. (A) Quantitative RTD-PCR for HCV RNA and serum ALT levels are shown. Two naive animals were inoculated with tupaia serum (using serum taken at 5 weeks postinoculation from Tup.5, originally inoculated with patient serum HCR6) containing 100 genome equivalents (GE)/ml and were monitored for 15 weeks postinoculation (Table 1). (B) Tupaia serum (taken at 10 weeks postinoculation from Tup.8, originally inoculated with RCV) that was positive for HCV RNA was passaged into two naive animals. The animals were inoculated with tupaia serum at 100 GE/animal and monitored for 15 weeks postinoculation. (C) Tupaia serum (taken at 8 weeks postinoculation from Tup.4, originally inoculated with RCV) that was positive for HCV RNA was passaged into naive animals. The animals were inoculated with serum at 100 GE/animal and monitored for 20 weeks postinoculation.

ulation titers (10^2 genome equivalents/animal) (Table 1). For Tup.11, serum from 4 weeks postinoculation contained almost 10^4 genome equivalents/ml of HCV RNA (Fig. 5B). In addition, significant increases in serum ALT accompanied detection of serum HCV RNA. These results indicate that HCV RNA-positive sera from group I actually contained infectious virion particles. They also suggest that reconstituted HCV particles made from cDNA are infectious in tupaias.

We amplified a portion of the NS5A sequence, which is known as the interferon sensitivity determining region, by reverse transcription-PCR as described in the supplemental material. Each PCR product was subcloned and sequenced to compare the encoded amino acid sequences. For the purposes of this study, animals were inoculated with a molecular clonal virus consisting of a unique viral sequence of cDNA. The interferon sensitivity determining region sequences recovered from an animal infected with clonal inoculum (Tup.8 at 103 weeks postinoculation) were found to be heterogeneous, with

a few amino acid substitutions (K2212M for 2/10 cases, L2232P for 1/10 cases, and L2253S for 6/10 cases) (see Fig. S2E in the supplemental material). Interestingly, the codon for amino acid 2224 encodes valine, but it was found to be variant for alanine and valine in sequences from the original patient serum (HCR6). Tupaias infected with patient serum also exhibited variability at position 2224; valine occupancy was rare, as was seen in the original HCR6 population (see Fig. S2B and C in the supplemental material). On the other hand, this position was occupied solely by valine for sequences recovered from Tup.8 (see Fig. S2E in the supplemental material), indicating that genetic variations shown for Tup.8 originated from the pHCR6 cDNA sequence. Taken together, quasispecies detection of circulating virus represents further evidence demonstrating intrinsic replication of HCV in tupaias despite low levels and infrequent detection of viremia.

DISCUSSION

In the present study, we described persistent HCV infection in tupaias. Long-term follow-up was performed and revealed histological progression of HCV-related liver disorders in infected tupaias, including steatosis, fibrosis, and cirrhosis, in addition to acute and chronic hepatitis. HCV genomic RNA was detected in animal sera intermittently throughout the entire course of infection. However, HCV RNA was detected in the liver upon sacrifice (3 years postinoculation). Furthermore, HCV RNA in serum contained genomic variants that had diverged from the inoculated virus (see Fig. S1 and S2 in the supplemental material). These data strongly indicate an established persistent infection in the tupaias studied. All animals exhibited HCV viremia soon after inoculation, yet the viremia was intermittent and accompanied by relatively low RTD-PCR titers compared with equivalent human and chimpanzee infections. The discrepancy between humans and tupaias might be due to host-dependent differences in replication efficiency. Over the course of HCV infection in these tupaias, serum ALT profiles indicated repeated liver injury, probably due to host immune responses mediated by agents such as cytotoxic T lymphocytes rather than direct viral cytopathic effects.

In cases of tupaia infection, experimental inoculations rarely led to sustained viremia, which for most human cases lasts for the entire course of infection. Even the course of infection appeared transient and self-resolved. It seems likely that HCV replication is less compatible with the tupaia host environment. This possibility was substantiated by a previous report by Xu et al. (34), where tissue-cultured virions of cloned genotype 1b, referred to as HCVcc in the paper, could not cause chronic infection with sustained viremia in tupaias. Although HCVcc actually infected most of the inoculated tupaias (83%; 10/12), chronic infection was seen for only a fraction of them (20%; 2/10). In this study, we also tried to detect a humoral response to HCV core antigen. We found that tupaia sera were HCV positive for antibodies only at occasional time points, observable as intermittent steep responses (data not shown). Overall, sustained seroconversion was not seen in this study, probably because HCV propagation in vivo was so limited or well controlled by host immunity. Given that models of HCV propagation are severely limited, the most important and interesting finding of this study is the successful detection of HCV RNA in livers of infected tupaias 3 years after inoculation, indicating that HCV persists in tupaias. Although the limited propagation of HCV in tupaias is a drawback of this model at the present time, the isolation of tupaia-adapted HCV may be feasible by performing multiple infection passages. This possibility is supported by both quasispecies development and successful reinfection.

The chimpanzee is the animal species most closely related to humans, and as a model, it has contributed significantly to our understanding of HCV infection and pathogenesis. However, reproducing HCV pathogenesis in humans or chimpanzees can take as long as 10 to 20 years. The chronically infected tupaias in the present study developed complicated liver disorders in a much shorter time. Using tupaias, with their relatively short life span (3 to 5 years in the laboratory), as a model of HCV infection, we can evaluate HCV pathogenesis and correlate senescence and duration of infection.

The recent development of a primary human hepatocyte xenograft-uPA/SCID mouse model opened up opportunities to test putative antivirals against HCV replication in vivo (10, 17). In this innovative model, human hepatocytes, which are transplanted into the lobe of a mouse liver, can support HCV replication effectively. As a result, the level of circulating HCV RNA is comparable to that of a human patient. However, this mouse model is immunodeficient, and thus, it lacks the interplay between host immunity and viral infection. Therefore, it does not provide a suitable platform for characterizing immune responses to HCV infection.

HCV infection in tupaias represents an important model of HCV infection, particularly for the study of key determinants controlling virus propagation in vivo. The pathogenesis of HCV infection can be substantially different among humans, chimpanzees, and tupaias, and the mechanisms governing these differences are of great interest. Comparative studies of HCV infection in these different species will help us to understand the basic mechanisms of persistent infection.

ACKNOWLEDGMENTS

We thank Masahiro Shuda for helpful assistance and Etsuko Endo for creating the figures. We also thank the staffs of the Departments of Microbiology and Cell Biology and Mitsugu Takahashi for breeding the tupaias.

This study was supported by grants from the Ministry of Education, Culture, Sports, Science and Technology of Japan; the Program for Promotion of Fundamental Studies in Health Sciences of the Pharmaceuticals and Medical Devices Agency of Japan; and the Ministry of Health, Labor and Welfare of Japan.

REFERENCES

1. **Abe, K., T. Kurata, Y. Teramoto, J. Shiga, and T. Shikata.** 1993. Lack of susceptibility of various primates and woodchucks to hepatitis C virus. J. Med. Primatol. **22:**433–434.
2. **Aoki, Y., H. Aizaki, T. Shimoike, H. Tani, K. Ishii, I. Saito, Y. Matsuura, and T. Miyamura.** 1998. A human liver cell line exhibits efficient translation of HCV RNAs produced by a recombinant adenovirus expressing T7 RNA polymerase. Virology **250:**140–150.
3. **Chomczynski, P., and N. Sacchi.** 1987. Single-step method of RNA isolation by acid guanidinium thiocyanate-phenol-chloroform extraction. Anal. Biochem. **162:**156–159.
4. **Choo, Q. L., G. Kuo, A. J. Weiner, L. R. Overby, D. W. Bradley, and M. Houghton.** 1989. Isolation of a cDNA clone derived from a blood-borne non-A, non-B viral hepatitis genome. Science **244:**359–362.
5. **Dash, S., G. Kalkeri, H. M. McClure, R. F. Garry, S. Clejan, S. N. Thung, and K. K. Murthy.** 2001. Transmission of HCV to a chimpanzee using virus

particles produced in an RNA-transfected HepG2 cell culture. J. Med. Virol. **65:**276–281.
6. **Flugge, P., E. Fuchs, E. Gunther, and L. Walter.** 2002. MHC class I genes of the tree shrew Tupaia belangeri. Immunogenetics **53:**984–988.
7. **Goldsmith, E. I.** 1978. The convention on international trade in endangered species of wild fauna and flora. J. Med. Primatol. **7:**122–124.
8. **Hong, Z., M. Beaudet-Miller, R. E. Lanford, B. Guerra, J. Wright-Minogue, A. Skelton, B. M. Baroudy, G. R. Reyes, and J. Y. Lau.** 1999. Generation of transmissible hepatitis C virions from a molecular clone in chimpanzees. Virology **256:**36–44.
9. **Hoofnagle, J. H.** 2002. Course and outcome of hepatitis C. Hepatology **36:**S21–S29.
10. **Inoue, K., T. Umehara, U. T. Ruegg, F. Yasui, T. Watanabe, H. Yasuda, J. M. Dumont, P. Scalfaro, M. Yoshiba, and M. Kohara.** 2007. Evaluation of a cyclophilin inhibitor in hepatitis C virus-infected chimeric mice in vivo. Hepatology **45:**921–928.
11. **Ishak, K., A. Baptista, L. Bianchi, F. Callea, J. De Groote, F. Gudat, H. Denk, V. Desmet, G. Korb, R. N. MacSween, et al.** 1995. Histological grading and staging of chronic hepatitis. J. Hepatol. **22:**696–699.
12. **Ito, T., K. Yasui, J. Mukaigawa, A. Katsume, M. Kohara, and K. Mitamura.** 2001. Acquisition of susceptibility to hepatitis C virus replication in HepG2 cells by fusion with primary human hepatocytes: establishment of a quantitative assay for hepatitis C virus infectivity in a cell culture system. Hepatology **34:**566–572.
13. **Kock, J., M. Nassal, S. MacNelly, T. F. Baumert, H. E. Blum, and F. von Weizsacker.** 2001. Efficient infection of primary tupaia hepatocytes with purified human and woolly monkey hepatitis B virus. J. Virol. **75:**5084–5089.
14. **Kolykhalov, A. A., E. V. Agapov, K. J. Blight, K. Mihalik, S. M. Feinstone, and C. M. Rice.** 1997. Transmission of hepatitis C by intrahepatic inoculation with transcribed RNA. Science **277:**570–574.
15. **Major, M. E., and S. M. Feinstone.** 1997. The molecular virology of hepatitis C. Hepatology **25:**1527–1538.
16. **Marcellin, P., T. Asselah, and N. Boyer.** 2002. Fibrosis and disease progression in hepatitis C. Hepatology **36:**S47–S56.
17. **Mercer, D. F., D. E. Schiller, J. F. Elliott, D. N. Douglas, C. Hao, A. Rinfret, W. R. Addison, K. P. Fischer, T. A. Churchill, J. R. Lakey, D. L. Tyrrell, and N. M. Kneteman.** 2001. Hepatitis C virus replication in mice with chimeric human livers. Nat. Med. **7:**927–933.
18. **Nascimbeni, M., E. Mizukoshi, M. Bosmann, M. E. Major, K. Mihalik, C. M. Rice, S. M. Feinstone, and B. Rehermann.** 2003. Kinetics of CD4+ and CD8+ memory T-cell responses during hepatitis C virus rechallenge of previously recovered chimpanzees. J. Virol. **77:**4781–4793.
19. **Pawlotsky, J. M.** 2002. Use and interpretation of virological tests for hepatitis C. Hepatology **36:**S65–S73.
20. **Ren, S., and M. Nassal.** 2001. Hepatitis B virus (HBV) virion and covalently closed circular DNA formation in primary tupaia hepatocytes and human hepatoma cell lines upon HBV genome transduction with replication-defective adenovirus vectors. J. Virol. **75:**1104–1116.
21. **Seeff, L. B.** 2002. Natural history of chronic hepatitis C. Hepatology **36:**S35–S46.
22. **Shimayama, T., S. Nishikawa, and K. Taira.** 1995. Generality of the NUX rule: kinetic analysis of the results of systematic mutations in the trinucleotide at the cleavage site of hammerhead ribozymes. Biochemistry **34:**3649–3654.
23. **Shimizu, Y. K., H. Igarashi, T. Kanematu, K. Fujiwara, D. C. Wong, R. H. Purcell, and H. Yoshikura.** 1997. Sequence analysis of the hepatitis C virus genome recovered from serum, liver, and peripheral blood mononuclear cells of infected chimpanzees. J. Virol. **71:**5769–5773.
24. **Shimizu, Y. K., A. Iwamoto, M. Hijikata, R. H. Purcell, and H. Yoshikura.** 1992. Evidence for in vitro replication of hepatitis C virus genome in a human T-cell line. Proc. Natl. Acad. Sci. USA **89:**5477–5481.
25. **Suh, Y. A., P. K. Kumar, K. Taira, and S. Nishikawa.** 1993. Self-cleavage activity of the genomic HDV ribozyme in the presence of various divalent metal ions. Nucleic Acids Res. **21:**3277–3280.
26. **Takeuchi, T., A. Katsume, T. Tanaka, A. Abe, K. Inoue, K. Tsukiyama-Kohara, R. Kawaguchi, S. Tanaka, and M. Kohara.** 1999. Real-time detection system for quantification of hepatitis C virus genome. Gastroenterology **116:**636–642.
27. **Tanaka, T., N. Kato, M. J. Cho, K. Sugiyama, and K. Shimotohno.** 1996. Structure of the 3′ terminus of the hepatitis C virus genome. J. Virol. **70:**3307–3312.
28. **Thomson, M., M. Nascimbeni, M. B. Havert, M. Major, S. Gonzales, H. Alter, S. M. Feinstone, K. K. Murthy, B. Rehermann, and T. J. Liang.** 2003. The clearance of hepatitis C virus infection in chimpanzees may not necessarily correlate with the appearance of acquired immunity. J. Virol. **77:**862–870.
29. **Tsukiyama-Kohara, K., N. Iizuka, M. Kohara, and A. Nomoto.** 1992. Internal ribosome entry site within hepatitis C virus RNA. J. Virol. **66:**1476–1483.
30. **Tsukiyama-Kohara, K., S. Tone, I. Maruyama, K. Inoue, A. Katsume, H. Nuriya, H. Ohmori, J. Ohkawa, K. Taira, Y. Hoshikawa, F. Shibasaki, M. Reth, Y. Minatogawa, and M. Kohara.** 2004. Activation of the CKI-CDK-Rb-E2F pathway in full genome hepatitis C virus-expressing cells. J. Biol. Chem. **279:**14531–14541.
31. **Walter, E., R. Keist, B. Niederost, I. Pult, and H. E. Blum.** 1996. Hepatitis B virus infection of tupaia hepatocytes in vitro and in vivo. Hepatology **24:**1–5.
32. **Wasley, A., and M. J. Alter.** 2000. Epidemiology of hepatitis C: geographic differences and temporal trends. Semin. Liver Dis. **20:**1–16.
33. **Xie, Z. C., J. I. Riezu-Boj, J. J. Lasarte, J. Guillen, J. H. Su, M. P. Civeira, and J. Prieto.** 1998. Transmission of hepatitis C virus infection to tree shrews. Virology **244:**513–520.
34. **Xu, X., H. Chen, X. Cao, and K. Ben.** 2007. Efficient infection of tree shrew (Tupaia belangeri) with hepatitis C virus grown in cell culture or from patient plasma. J. Gen. Virol. **88:**2504–2512.
35. **Yanagi, M., R. H. Purcell, S. U. Emerson, and J. Bukh.** 1997. Transcripts from a single full-length cDNA clone of hepatitis C virus are infectious when directly transfected into the liver of a chimpanzee. Proc. Natl. Acad. Sci. USA **94:**8738–8743.
36. **Yanagi, M., M. St Claire, M. Shapiro, S. U. Emerson, R. H. Purcell, and J. Bukh.** 1998. Transcripts of a chimeric cDNA clone of hepatitis C virus genotype 1b are infectious in vivo. Virology **244:**161–172.
37. **Zhao, X., Z. Y. Tang, B. Klumpp, G. Wolff-Vorbeck, H. Barth, S. Levy, F. von Weizsacker, H. E. Blum, and T. F. Baumert.** 2002. Primary hepatocytes of Tupaia belangeri as a potential model for hepatitis C virus infection. J. Clin. Invest. **109:**221–232.

Journal of Medical Virology 82:1545–1553 (2010)

Natural Killer Cells Target HCV Core Proteins During the Innate Immune Response in HCV Transgenic Mice

Kenichi Satoh,[1,2] Hiroki Takahashi,[2] Chiho Matsuda,[1] Toshiyuki Tanaka,[3] Masayuki Miyasaka,[4] Mikio Zeniya,[2] and Michinori Kohara[1]*

[1]*Department of Microbiology and Cell Biology, The Tokyo Metropolitan Institute of Medical Science, Bunkyo-ku, Tokyo, Japan*
[2]*Division of Gastroenterology and Hepatology, Department of Internal Medicine, The Jikei University School of Medicine, Minato-ku, Tokyo, Japan*
[3]*Laboratory of Immunobiology, Department of Pharmacy, School of Pharmacy, Hyogo University of Health Sciences, Chuo-ku, Kobe, Japan*
[4]*Laboratory of Immunodynamics, Department of Microbiology and Immunology, Osaka University Graduate School of Medicine, Suita, Osaka, Japan*

The mechanism of the innate immune response to hepatitis C virus (HCV) has not been fully elucidated, largely due to the lack of an appropriate model. We used HCV transgenic (Tg) mice, which express core, E1, E2, and NS2 proteins regulated by the Cre/*loxP* switching expression system, to examine the innate immune response to HCV structural proteins. Twelve hours after HCV transgene expression, HCV core protein levels in Tg mouse livers were 15–47 pg/mg. In contrast, in Tg mice with a depletion of natural killer (NK) cells, we observed much higher levels of HCV core proteins (1,597 pg/ml). Cre-mediated genomic DNA recombination efficiency in the HCV-Tg mice was strongly observed in NK cell-depleted mice between 0.5 and 1 day as compared to non-treated mice. These data indicated that NK cells participate in the elimination of core-expressing hepatocytes in the innate immune responses during the acute phase of HCV infection. ***J. Med. Virol. 82:1545–1553, 2010.***

KEY WORDS: HCV; Cre/loxP switching Tg; innate immunity; natural killer cell; core protein

INTRODUCTION

Although a variety of studies have demonstrated that infection with hepatitis C virus (HCV) elicits an innate immune response in human hosts, the mechanisms behind this response are not well understood. Details on the first step of the immune process might assist in the development of treatments for chronic hepatitis, cirrhosis, and hepatocellular carcinoma. One of the factors limiting such HCV immune research is the general lack of animal models: Humans are the only natural HCV host, and to date, chimpanzees are the only animals that have been infected with HCV.

Clinically, approximately 50% of symptomatic patients eliminate the virus, whereas in an asymptomatic course, more than 80% of acute HCV infections develop into chronic infection [Gerlach et al., 2003], indicating that the infected host's immune reaction may influence the course of the disease. In the chimpanzee model, HCV significantly induces type I interferon (IFN) [Bigger et al., 2001; Su et al., 2002]. However, this response occurs irrespective of the outcome of infection [Disson et al., 2004; Machida et al., 2001; Su et al., 2002; Thimme et al., 2002], and NS3-4A can inhibit RIG-1-mediated signaling, which is required to be activated for IFN production [Vilasco et al., 2006].

Natural killer (NK) cells constitute the first line of host defense against invading pathogens and are usually activated in the early phase of viral infection.

Abbreviations used: HCV, hepatitis C virus; NK cell, natural killer cell; IFN, interferon; Tg, transgenic; ALT, alanine aminotransferase; IRF, interferon regulatory factor.

Grant sponsor: Ministry of Education, Culture, Sports, Science and Technology of Japan; Grant sponsor: Program for Promotion of Fundamental Studies in Health Sciences of the National Institute of Biomedical Innovation of Japan; Grant sponsor: Ministry of Health, Labor and Welfare of Japan.

*Correspondence to: Michinori Kohara, PhD, Department of Microbiology and Cell Biology, The Tokyo Metropolitan Institute of Medical Science, 2-1-6 Kamikitazawa, Setagaya-ku, Tokyo 156-8506, Japan. E-mail: kohara-mc@igakuken.or.jp

Accepted 28 April 2010
DOI 10.1002/jmv.21859
Published online in Wiley InterScience (www.interscience.wiley.com)

The liver is particularly enriched with NK cells, which are activated by hepatotropic viruses such as HCV. There have been some reports of the association between NK cells and HCV [Ebihara et al., 2008; Knapp et al., 2009; Vidal-Castineira et al., 2010]. For instance, NK cell numbers were consistently lower in individuals with persistent HCV infections [Golden-Mason et al., 2008]. Additionally, the function of NK cells can be inhibited by HCV proteins such as envelope protein E2, which impairs the effector function of NK cells by interacting with CD81 on their surface [Crotta et al., 2002; Tseng and Klimpel, 2002].

Most of these studies on the association between NK cells and HCV have been performed during the chronic phase of HCV infection. To our knowledge, there has been no research on the innate immune response during the acute phase of HCV infection, because of the difficulty in analyzing early immune reactions and the lack of appropriate animal models. Here, we have overcome this difficulty by using the Cre/*loxP* system to create a mouse model with conditional HCV transgene expression. This allowed us to analyze HCV-specific innate immunity.

MATERIALS AND METHODS

HCV Transgenic Mice

HCV-Tg mice CN2-8 and CN2-29 (BALB/c, 9- to 12-week old) were used in the experiments. These two Tg mice lineages possess HCV genotype 1b, which is regulated by the Cre/*loxP* conditional switching system [Wakita et al., 1998]. NK cell- and $CD8^+$ T-cell-deficient HCV-Tg mice were also established by mating HCV-Tg mice with syngenic IRF-1-deficient mice, in which a strong reduction in NK cells [Duncan et al., 1996; Ohteki et al., 1998] and $CD8^+$ T cells [Matsuyama et al., 1993] has been reported.

All mice were cared for according to the guidelines of the NIH Guide for the Care and Use of Laboratory Animals.

Structure of CALCN2, the Cre-Mediated Activation Transgene Unit

R6CN2 HCV cDNA (nucleotides: 294–3,435, aa: 1–1,013) contains the core, E1, E2, and NS2 regions. This construct does not lead to HCV mRNA transcription before recombination. It was cloned downstream of the CAG promoter, neomycin-resistant gene (*neo*), and poly(A) signal; the latter two of these were flanked by *loxP* sequences. The CAG promoter comprises, in order, the cytomegalovirus enhancer, actin promoter, and the globin poly(A) signal. CALNCN2, the Cre-mediated activation transgene unit, consists of the CAG promoter, a *loxP* sequence, the *neo*-resistance gene, the SV40 poly(A) signal, a second *loxP* sequence, R6CN2 HCV cDNA, and the globin poly(A) signal, in that order.

Upon recognition of the *loxP* site, Cre recombinase deletes the neo gene and the SV40 poly(A) signal, along with one of the *loxP* sequences. It then ligates the CAG promoter to the HCV cDNA and the globin poly(A) signal. This genomic structure alteration enables the production of HCV mRNA [Wakita et al., 1998].

Hydrodynamics-Based Transfection of Naked Plasmid DNA

Cre recombinase cDNA (pCAN-Cre/pBR325 plasmid) was cloned downstream of the CMV promoter. Plasmid DNA was prepared using the triton-cesium chloride method. Plasmid DNA (20 μg) was diluted with 2.0 ml of PBS(−) mixed with atelocollagen (KOKENCELLGEN I-AC; Koken, Tokyo, Japan) [Ochiya et al., 2001; Minakuchi et al., 2004] to a final concentration of 0.01%. This was then injected via a tail vein, after which it entered circulation within 6–8 sec [Liu et al., 1999].

Depletion of NK Cells

Transgenic mice were treated intraperitoneally with 1 mg of anti-IL2 receptor-β monoclonal antibody (TM-βI, rat IgG2b) [Tanaka et al., 1993] in 500 μl of PBS(−) once, 2 days before Cre/loxP switching.

Quantification of HCV Core Proteins in Mouse Livers

Hepatocyte HCV core protein concentrations were quantified with a fluorescent enzyme immunoassay (FEIA) by using HCV core monoclonal antibodies from a commercial kit, as previously described [Kashiwakuma et al., 1996].

Immunoblot Analysis

Liver tissues (100–150 μg) were lysed with 300 μl of RIPA buffer (1% SDS, 0.5% Nonidet P40, 0.5 mmol/L EDTA,150 mmol/L NaCl, and 1 mmol/L DTT and 10 mmol/L Tris, pH 7.4). After the supernatant protein concentration was determined, 30 μg of total protein was electrophoresed on SDS–PAGE (15% polyacrylamide) and transferred to a polyvinylidene difluoride (PVDF) membrane (Immobilon-P, Millipore, Bedford, MA). The membrane was incubated with biotinylated 515S (an anti-HCV core monoclonal antibody), 384 (an anti-HCV E1 monoclonal antibody), or 541 (an anti-HCV E2 monoclonal antibody) [Tsukiyama-Kohara et al., 2004], followed by horseradish peroxidase-conjugated streptavidin. Proteins were visualized using the ECL system (Amersham Biosciences, Cleveland, OH).

Southern Blotting

Genomic DNA (4 μg) was extracted from mouse liver tissue by using the phenol–chloroform method. It was digested with *Xba*I and then resolved by electrophoresis on a 0.8% agarose gel. Bands were transferred to a Hybond-N membrane (Amersham Biosciences) by using the Vacugene 2016 (LKB Biotechnology, Bromma, Sweden). The blots were then probed with a ^{32}P-dCTP-

labeled CALNCN2 (nucleotides: 483–1,389) probe. The probe was generated using a Random Primer DNA Labeling Kit, Ver 2.0 (Takara, Shiga, Japan).

Northern Blotting

Total RNA (30 μg) was extracted from mouse liver tissue by using the AGPC method. Bands were transferred to a Hybond-N membrane (Amersham Biosciences). The blots were then probed with the same probe used for Southern blotting.

Expression Plasmids of HCV Structural Proteins

We generated expression plasmids of HCV-core (aa: 1–192; pEF-core), HCV-E1 (aa: 168–383; pEF-E1), and HCV-E2 (aa: 367–830; pEF-E2) [Takaku et al., 2003] under the control of the EF2-α promoter, and HCV-CN2 (aa: 1–1,013; pCAL CN2) [Tsukiyama-Kohara et al., 2004] and β-lactamase (pCAL-LacZ), under the control of the CAG promoter.

Cytokine Assay

Secretion of serum IFN-γ [Carroll et al., 1997], IL-12, and TNF-α was measured using enzyme-linked immunosorbent assay kits (BioSource, Camarillo, CA), according to the manufacturer's protocols.

Assay of Alanine Aminotransferase (ALT) Levels

Serum ALT concentrations were determined with a Transferase Nissui kit (Nissui Pharmaceutical Co., Tokyo, Japan) and then standardized and expressed as IU/L.

RESULTS

HCV Core Protein and ALT Levels During the Early Phase of HCV Transgenic Mouse

In CN2-8 Tg mice, HCV core protein expression levels were as follows: day 0.5: 15 ± 16 pg/mg; day 1: 175 ± 96 pg/mg; day 2: 207 ± 77 pg/mg; day 3: 33 ± 41 pg/mg; day 4: 431 ± 256 pg/mg; day 14: 4 ± 1 pg/mg (Fig. 1A). In the CN2-29 Tg mice, HCV core protein expression levels were as follows: day 0.5: 47 ± 13 pg/mg; day 1: 495 ± 165 pg/mg; day 2: 1189 ± 210 pg/mg; day 3: 26 ± 39 pg/mg; day 4: 59 ± 49 pg/mg; day 14: 2 ± 2 pg/mg (Fig. 1B). ALT levels were 489 ± 150 IU/L in the CN2-8 Tg mice and 2,282 ± 358 IU/L in the CN2-29 Tg mice at day 0.5, after which the levels quickly decreased. In both mice lineages, HCV core protein expression levels were low from day 8. In contrast, HCV core protein was not detected and the ALT levels were low (357 ± 150 IU/L) at day 0.5 in the CN2-29 Tg mice injected with the negative control vector (pBR325) (Fig. 1C).

In the immunoblot analysis, the HCV core (21 kDa) protein was detectable from days 0.5 to 3 (Fig. 1D). To investigate why the core protein was eliminated after day 3, we performed Southern and Northern blot analyses using liver tissue extracts. Transgene recombination occurred in the Tg mouse livers (Fig. 1E). CALNCN2 mRNA expression levels were similar throughout the study period (Fig. 1F). Although HCV mRNA was consistently observed, the HCV core protein was eliminated by day 4 (Fig. 1D), suggesting that some immune factors were active against HCV core protein from day 3 onward.

Histopathology of the HCV Protein Expressed During the Early Phase of HCV Transgenic Mouse

Histopathology of the CN2-29 Tg mice (Fig. 2B–E) revealed inflammation and elevation of ALT levels in livers with HCV structural protein expression compared to that in livers without HCV structural protein expression (Fig. 2F–I). The presence of HCV structural proteins was associated with the following: hepatocyte necrosis and mononuclear cell infiltration in both the liver lobules and in the periportal area, on day 0.5 (Fig. 2B); mononuclear cell infiltration, on days 1 (Fig. 2C) and 3 (Fig. 2E); and Kupffer-like infiltrated cells, on day 2 Fig. 2D). No changes in inflammation were found in the control vector-injected mice (Fig. 2F–I).

NK Cell Activity Against Cells Expressing HCV Proteins

HCV core protein expression levels were higher in the CN2-8 IRF-1 knockout mice than in wild-type Tg mice (309 ± 76 pg/mg vs. 15 ± 16 pg/mg), while ALT levels were lower (194 ± 53 I/U vs. 489 ± 142 IU/L; Fig. 1A).

HCV core protein expression levels were higher in NK cell-depleted mice with anti-IL2 receptor-β antibodies than in non-treated CN2-29 Tg mice (1,597 ± 153 pg/mg vs. 47 ± 13 pg/mg), while ALT levels were lower (608 ± 258 IU/L vs. 2,282 ± 458 IU/L) on day 0.5 (Figs. 1B and 3). However, core protein levels were drastically reduced in the treated mice on day 2. Transgene recombination was strongly observed between days 0.5 and 1 (Fig. 3C), indicating that activated NK cells were responsible for eradicating the HCV proteins.

In BALB/c mice whose livers had been hydrodynamically transfected with the pCAL-CN2 plasmid, HCV core protein expression level was 123 ± 45 pg/mg and the ALT level was 3,256 ± 703 IU/L on day 0.5. By day 1, both the HCV core protein expression level (54 ± 65 pg/mg) and the ALT level (841 ± 174 IU/L) had decreased; they were also relatively low on day 2 (Fig. 4A).

Both the HCV core protein expression level (2,900 ± 400 pg/mg on days 0.5 and 10,700 ± 3,100 pg/mg on day 1) and the ALT level (295 ± 197 IU/L on day 0.5 and 91 ± 51 IU/L on day 1) were lower in IRF-1 knockout BALB/c mice than in wild-type BALB/c mice (Fig. 4A,B). In contrast, in wild-type BALB/c mice hydrodynamically transfected with the pCAL-LacZ plasmid, the β-galactosidase level did not dramatically change over the study period (7.9 ± 2.0 on day 0.5; 3.9 ± 2.1 on day 14). The ALT level (450 ± 90 IU/L) was lower in plasmid-transfected mice than in wild-type mice (Fig. 4A,C), but

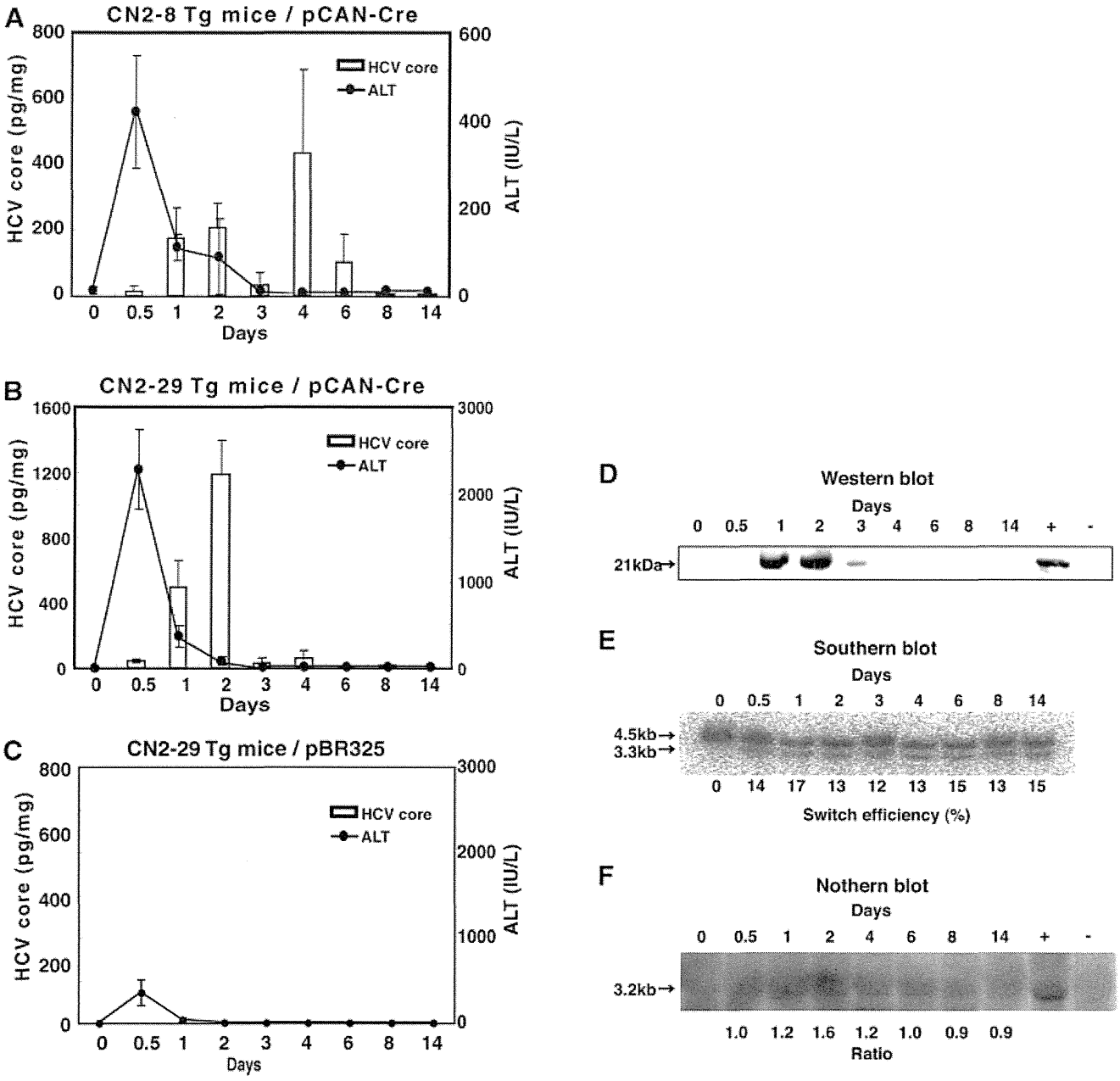

Fig. 1. Quantification of HCV core protein production and ALT levels in transgenic mice hydrodynamically transfected with the pCAN-Cre plasmid. Values for core protein and serum ALT levels represents the mean and SD from three experiments. **A**: CN2-8 transgenic mice. Analysis of quantity of core protein and serum ALT levels in the hepatocytes. Hepatitis was first detectable via elevated serum ALT activity on day 0.5, after which ALT activity rapidly rose, only to return to the baseline level after day 3. Hepatocyte core protein levels peaked twice, on day 2 (207 ± 77 pg/mg) and day 4 (431 ± 256 pg/mg). **B**: CN2-29 transgenic mice. Hepatitis was first detectable as elevated serum ALT activity on day 0.5. Serum ALT activity peaked at $2{,}282 \pm 358$ IU/L and then declined gradually from day 1 (366 ± 123 IU/L). It returned to the baseline level after day 2. Hepatocyte core protein levels were first detectable on day 0.5 (47 ± 13 pg/mg), peaked on day 2 ($1{,}189 \pm 210$ pg/mg), and returned to the baseline level after day 3. **C**: Serum ALT levels in negative control plasmids (pBR325, 20 μg) injected into CN2-29 transgenic mice. The serum ALT level of the control plasmids was lower than in CN2-29 transgenic mice and was only detectable on day 0.5, after which it returned to the baseline level. Core protein levels were not detectable. **D**: Immuno-blot from the liver of a CN2-29 transgenic mouse liver hydrodynamically transfected with the pCAN-Cre plasmid. HCV core protein in the liver extract was barely detectable 12 h after switching in the CN2-29 Tg mouse, was strongly detected on days 1 and 2, and was eliminated after day 3. The density of the HCV core protein band reflected the HCV protein expression levels shown in Fig. 1B. **E**: Switching efficiency of Cre-mediated genomic DNA recombination in the liver of a CN2-29 transgenic mouse hydrodynamically transfected with the pCAN-Cre plasmid. HCV transgene recombination in the somatic tissues of pCANCre-injected mice. Southern blot analysis of tissues from CN2-29 mice. Transgene recombination was consistently observed between days 0.5 and 14. kb, kilobase pairs. **F**: Cre-mediated genomic DNA recombination and mRNA in the CN2-29 transgenic mouse liver hydrodynamically transfected with the pCAN-Cre plasmid. The expression level of CALNCN2 mRNA by Northern blot analysis.

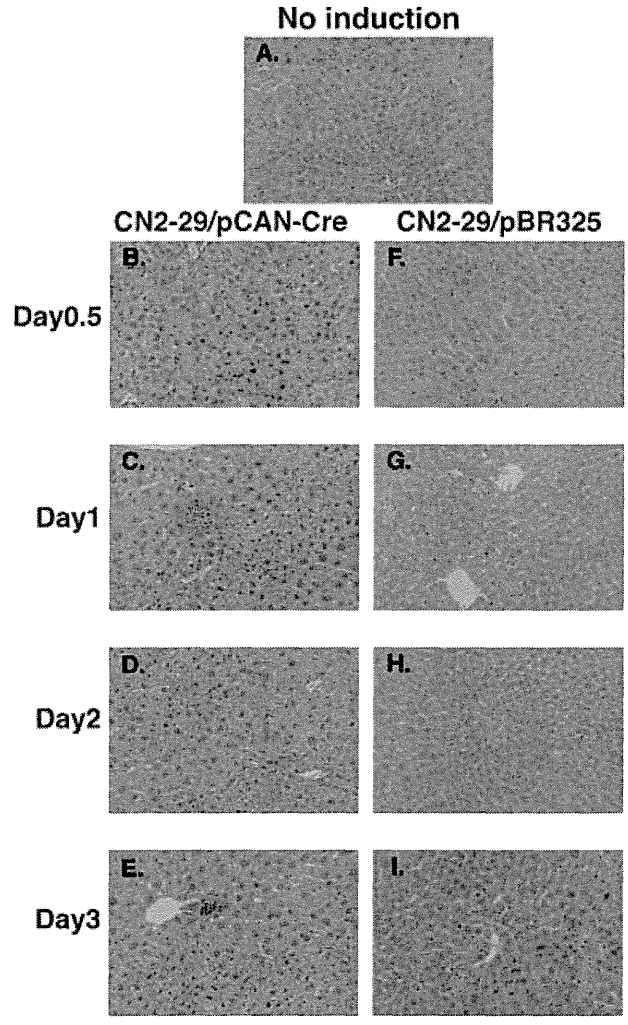

Fig. 2. Hematoxylin and eosin staining of liver sections from CN2-29 Tg mice. The presence of HCV structural proteins was associated with the following: (**B**) hepatocyte necrosis and mononuclear cell infiltration in the liver lobules and periportal area on day 0.5; (**C,E**) mononuclear cell infiltration on days 1 and 3; (**D**) Kupffer-like cell infiltration on day 2. **F–I**: No inflammation changes were seen in the liver following pBR325 plasmid injection.

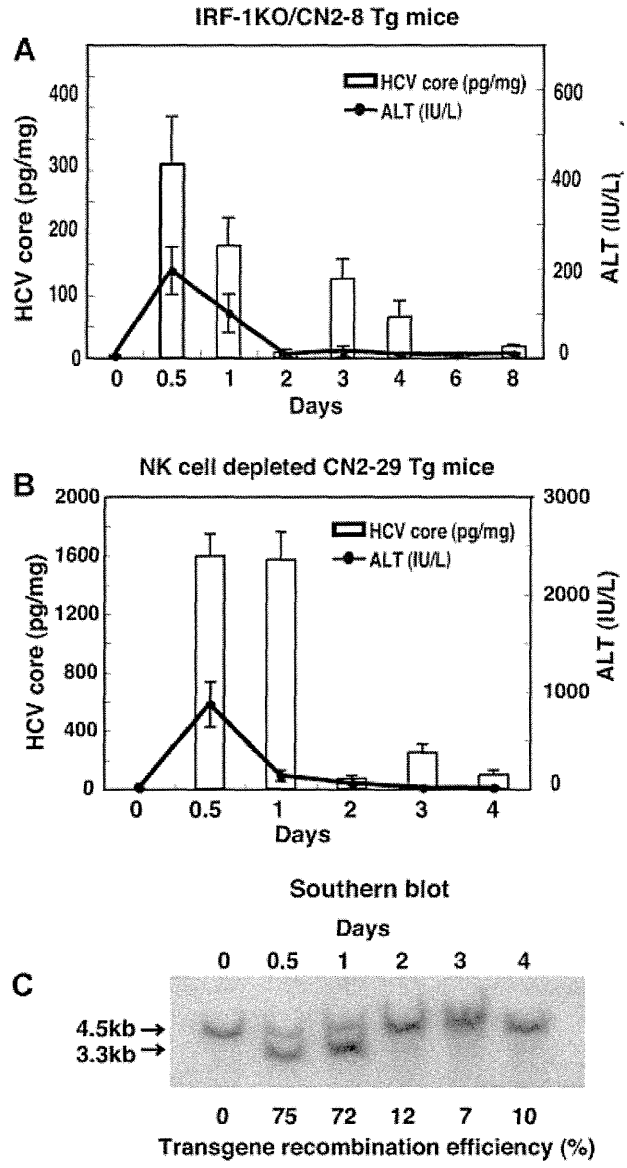

Fig. 3. Quantification of HCV core protein production and serum ALT levels in IRF-1 knockout CN2-8 transgenic mice and NK cell-depleted CN2-29 transgenic mice hydrodynamically transfected with the pCAN-Cre plasmid. **A**: HCV core protein and serum ALT levels in IRF-1 knockout CN2-8 Tg mice. The core protein level in the hepatocytes rapidly increased on day 0.5 (309 ± 76 pg/mg). The serum ALT level (194 ± 53 IU/L) was lower than in wild-type mice (490 ± 150 IU/L) on day 0.5 (Fig. 1A). **B**: HCV core protein and serum ALT levels in NK cell-depleted CN2-29 Tg mice. The core protein level in the liver rapidly increased on day 0.5 ($1{,}597 \pm 153$ pg/mg). The serum ALT level (489 ± 142 IU/L) was lower than in wild-type mice ($2{,}282 \pm 358$ IU/L) on day 0.5 (Fig. 1B). **C**: Cre-mediated genomic DNA recombination efficiency throughout the study period.

the β-galactosidase level (7.4 ± 2.5 on day 0.5 and 5.4 ± 2.3 on day 1) was comparable. Finally, the ALT level was 325 ± 178 IU/L on day 0.5 (Fig. 4D).

When the pCAN-Cre/pBR325 plasmid was injected into wild-type BALB/c mice, the results were similar to those seen in the absence of the vector (data not shown), suggesting that the pCAN-Cre plasmid injection had no effect.

Cumulatively, these findings suggest that HCV protein-expressing cells were eliminated by NK cells during the acute early phase of innate immunity.

IFN-γ Secretion Induced HCV Core Protein in the Acute Early Phase of Innate Immunity

We analyzed cytokine (IFN-γ, IL-12, and TNF-α levels from days 0 to 14 after the hydrodynamic transfection of pCAN-Cre plasmids into CN2-29 Tg mice. Serum IL-12 and TNF-α were not detected on any day during the study period (data not shown). Serum IFN-γ was detected on day 0.5 in pCAN-Cre-transfected mice, but not in control vector-injected mice (Fig. 5A).

IFN-γ was strongly secreted on day 0.5 in response to transfection with pEF-core expression plasmids (Fig. 5B), but was only slightly induced by the HCV E1 and E2 (not detected) proteins (Fig. 5B). In contrast,

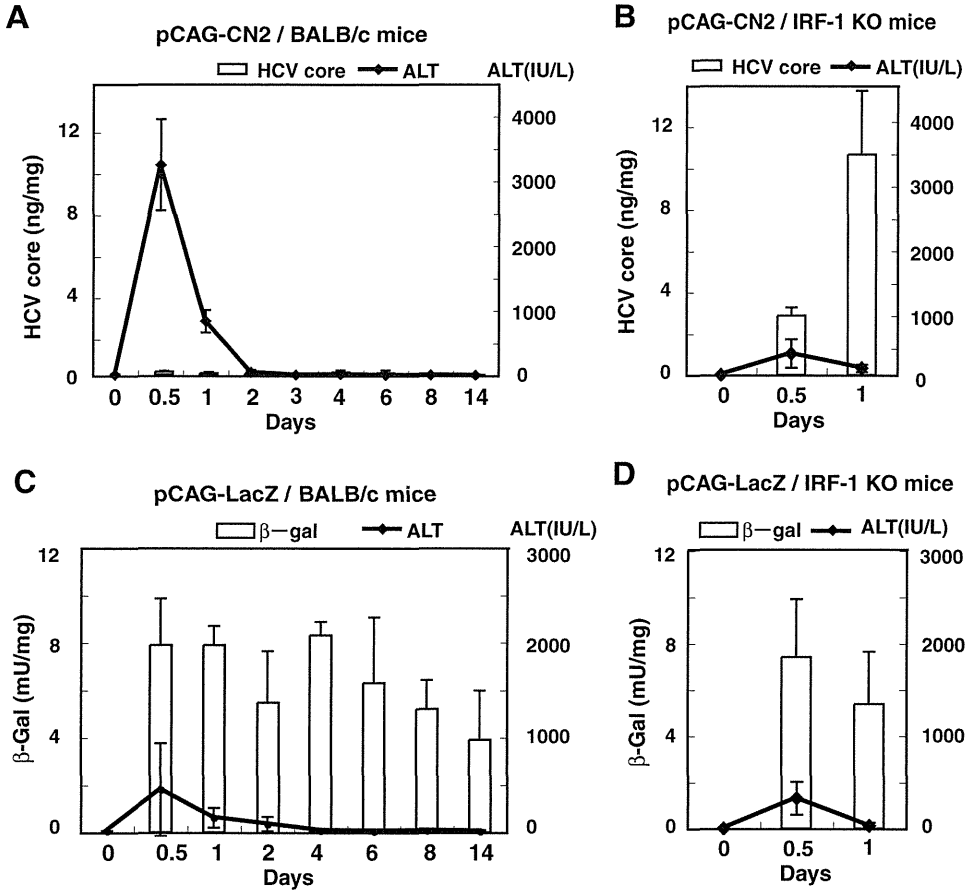

Fig. 4. Quantification of HCV core protein production and serum ALT levels in wild-type BALB/c mice and IRF-1 knockout BALB/c mice hydrodynamically transfected with expression plasmids. **A**: Results for wild-type BALB/c mice injected with pCAG-CN2 (Fse). HCV core protein in the liver was barely detectable at day 0.5 (0.123 ± 0.045 ng/mg) and declined gradually thereafter. The serum ALT level peaked on day 0.5 (3,256 ± 703 IU/L) and declined gradually thereafter. **B**: Results for IRF-1 knock out BALB/c mice injected with pCAG-CN2 (Fse). HCV core protein levels in the hepatocytes was most strongly detected on days 0.5 (2.9 ± 0.4 ng/mg) and 1 (10.7 ± 3.1 ng/mg). Serum ALT was suppressed on day 0.5 (295 ± 197 IU/L). **C**: Results for BALB/c mice injected with pCAG-LacZ. Liver β-gal levels were first detectable on day 0.5 (7.9 ± 2.0 mU/mg) and were consistently detectable until day 14 (3.9 ± 2.1 mU/mg). The serum ALT level (450 ± 490 IU/L) was lower than that shown in Figure 2A (3,256 ± 703 IU/L) at day 0.5, and returned to the baseline level after day 2. **D**: Results from IRF-1 knockout BALB/c mice injected with pCAG-LacZ. Liver β-gal levels were detected on days 0.5 (7.4 ± 2.5 mU) and 1 (5.4 ± 2.3 mU). The serum ALT level was (352 ± 178 IU/L) on day 0.5.

serum IFN-γ was not detected after transfection with pEF-core expression plasmids in CN2-8 IRF-1 (Fig. 5C). Serum IFN-γ secretion was suppressed in NK cell-depleted CN2-29 Tg mice and was not stimulated by pCAL-LacZ plasmid injection (Fig. 5D,E).

DISCUSSION

Immune responses to HCV during the acute phase of infection might play a crucial role in determining whether HCV is eliminated or is able to persist in the body. However, acute HCV infection is rarely symptomatic, making it tremendously difficult to analyze in vivo. In the present study, we generated an acute HCV model for the first time by using Tg mice with conditional expression regulated by the Cre/*loxP* system. Because there were no viral vector effects, we were able to observe HCV-specific innate immunity by using hydrodynamic transfection techniques.

NK cells constitute the first line of host defense against invading pathogens. Activated NK cells play an essential role in recruiting virus-specific T cells and inducing antiviral immunity in the liver [French et al., 2003]. They also eliminate virus-infected hepatocytes directly by cytolytic mechanisms and indirectly by secreting cytokines, which induce an antiviral state in host cells. In vitro studies revealed that NK cells are activated by cytokines during acute HCV infection [Yoon et al., 2008] and play an important antiviral role by eliminating the virus, both by killing it directly and by producing cytokines such as IFN-γ [Golden-Mason and Rosen, 2006].

In the present study, hepatocyte necrosis and intrahepatic mononuclear cell infiltration were observed on days 0.5 and 1 in wild-type mice. These were associated with elevated levels of serum ALT and IFN-γ and with reduced levels of HCV core protein expression. In contrast, NK cell depletion by IRF-1 knockout or treatment with anti-IL-2 receptor-β antibody was

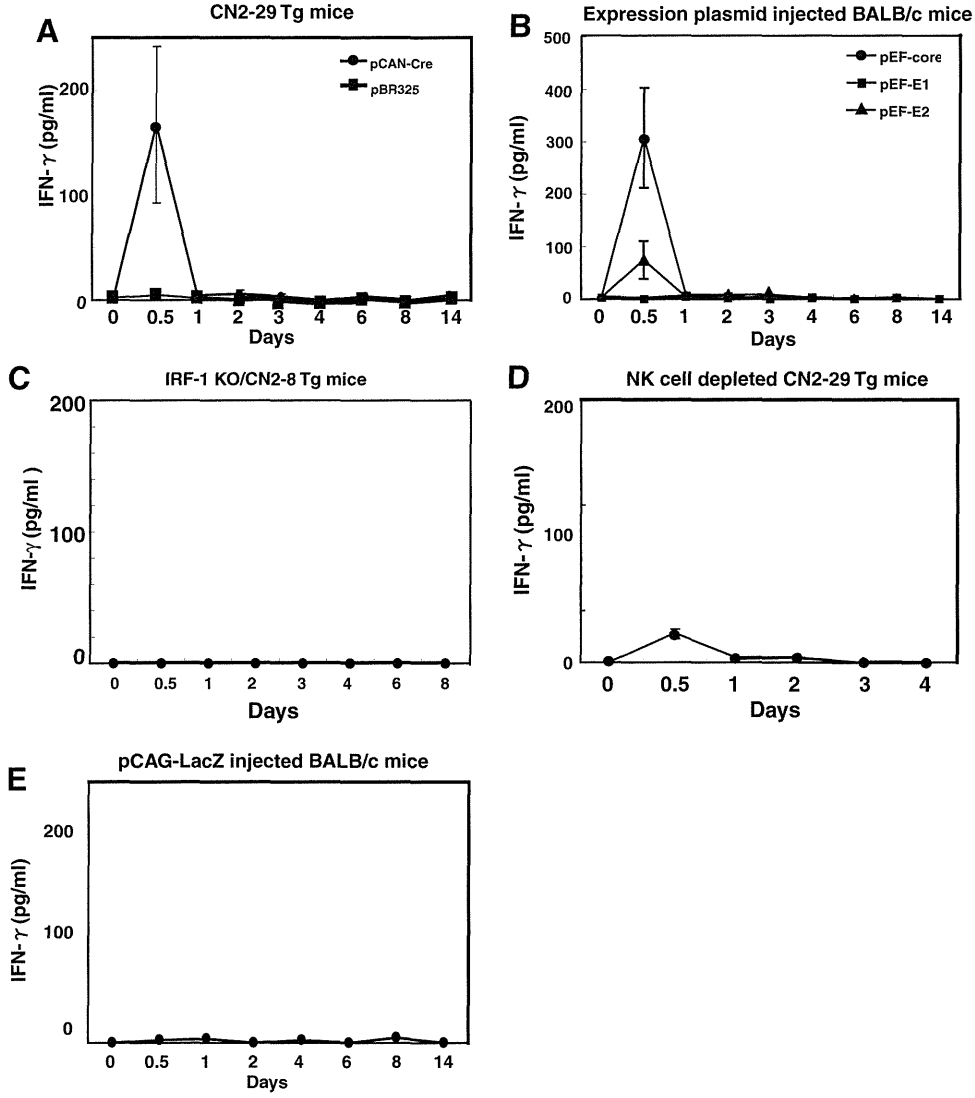

Fig. 5. Serum IFN-γ levels. **A**: Serum IFN-γ levels in CN2-29 Tg mice injected with the pCAN-Cre plasmid. Serum IFN-γ (168 ± 62 pg/ml) was detectable on day 0.5 in the pCAN-Cre plasmid-injected CN2-29 Tg mice (circle), but was not detectable in the pBR325 plasmid-injected CN2-29 Tg mice (square). **B**: Serum IFN-γ levels in mice injected with pEF-core (circle), -E1 (square), and -E2 (triangle) plasmids. **C**: Serum IFN-γ levels in IRF-1 knockout CN2-8 Tg mice injected with the pCAN-Cre plasmid. **D**: Serum IFN-γ levels in NK cell-depleted CN2-29 Tg mice injected with the pCAN-Cre plasmid. **E**: Serum IFN-γ levels in BALB/c mice injected with the pCAL-LacZ plasmid.

accompanied by increases in HCV core protein expression and decreased levels of ALT and IFN-γ on days 0.5 and 1. These results were confirmed by our histological observations. Cumulatively, these data suggest that the activity of NK cells might be directly cytolytic; specifically, they appear to play a significant role in IFN-γ secretion and elimination of virus-infected hepatocytes—especially core protein-presented hepatocytes—during the early phase of infection (days 0–1). Since the number of CD8+ cytotoxic T cells is greatly reduced in CN2-8 IRF-1 knockout mice, T cells usually participate in innate immunity, rather than acquired immunity. It has previously been reported that NK cells are required to recruit virus-specific T cells in response to HCV infection [Ahmad and Alvarez, 2004; Irshad et al., 2008]. These reports, together with our current work, indicate that NK cells play a very important antiviral role during acute HCV infection.

According to the results of the Southern and Northern blot analyses, non-cytolytic HCV core protein elimination takes place from days 3 to 14. However, this does not appear to be associated with IFN-γ or CD8+ cytotoxic T cells. Thus, during this period, another immune factor might be involved in eliminating HCV core protein in the hepatocytes without elevating ALT activity.

It is interesting that HCV core protein, but not E1 or E2 protein, induced the elevation of IFN-γ. Since HCV core protein is reported to activate NF-kB, thereby inducing the cellular inflammatory response [Dolganiuc et al., 2004], there is a possibility that HCV core protein

itself participates in the elevation of IFN-γ. IFN-γ is known to be expressed in the liver when infections spontaneously clear [Major et al., 2002; Thimme et al., 2002] and to be involved in the non-cytolytic control of HCV-infected hepatocytes [Thimme et al., 2001]. Additionally, IFN-γ inhibits the replication of subgenomic HCV replicons [Lohmann et al., 1999; Blight et al., 2000] in tissue culture cells [Frese et al., 2002; Lanford et al., 2003]. Since NK cells produce a large amount of IFN-γ when they are activated in response to inflammation, such as that caused by acute viral infection, both NK cells and IFN-γ may contribute to the innate immune response during acute HCV infection.

In conclusion, this Tg mouse model permits analysis of the HCV-specific immune response while avoiding adenovirus which has been applied for the study of HCV immunity. By using this model, we could determine some of the potential roles of NK cells in response to the presence of HCV structural protein during the early naïve phase of HCV infection. These findings confirm that NK cell activity is crucial in eliminating HCV-infected hepatocytes. This suggests that a potential new therapeutic approach is activation of NK cells in order to restore the innate immune defenses that control HCV replication.

ACKNOWLEDGMENTS

The authors wish to express their gratitude to Izumu Saito for his kind gift of the pCAN-Cre plasmid. We thank Dr. Masahiro Shuda for helpful comments during the preparation of this manuscript. We also thank Mitsugu Takahashi for breeding the transgenic mice.

REFERENCES

Ahmad A, Alvarez F. 2004. Role of NK and NKT cells in the immunopathogenesis of HCV-induced hepatitis. J Leukoc Biol 76:743–759.

Bigger CB, Brasky KM, Lanford RE. 2001. DNA microarray analysis of chimpanzee liver during acute resolving hepatitis C virus infection. J Virol 75:7059–7066.

Blight KJ, Kolykhalov AA, Rice CM. 2000. Efficient initiation of HCV RNA replication in cell culture. Science 290:1972–1974.

Carroll JM, Crompton T, Seery JP, Watt FM. 1997. Transgenic mice expressing IFN-gamma in the epidermis have eczema, hair hypopigmentation, and hair loss. J Invest Dermatol 108:412–422.

Crotta S, Stilla A, Wack A, D'Andrea A, Nuti S, D'Oro U, Mosca M, Filliponi F, Brunetto RM, Bonino F, Abrignani S, Valiante NM. 2002. Inhibition of natural killer cells through engagement of CD81 by the major hepatitis C virus envelope protein. J Exp Med 195:35–41.

Disson O, Haouzi D, Desagher S, Loesch K, Hahne M, Kremer EJ, Jacquet C, Lemon SM, Hibner U, Lerat H. Impaired clearance of virus-infected hepatocytes in transgenic mice expressing the hepatitis C virus polyprotein. Gastroenterology 2004. 126:859–872.

Dolganiuc A, Oak S, Kodys K, Golenbock DT, Finberg RW, Kurt-Jones E, Szabo G. 2004. Hepatitis C core and nonstructural 3 proteins trigger toll-like receptor 2-mediated pathways and inflammatory activation. Gastroenterology 127:1513–1524.

Duncan GS, Mittrucker HW, Kagi D, Matsuyama T, Mak TW. 1996. The transcription factor interferon regulatory factor-1 is essential for natural killer cell function *in vivo*. J Exp Med 184:2043–2048.

Ebihara T, Shingai M, Matsumoto M, Wakita T, Seya T. 2008. Hepatitis C virus-infected hepatocytes extrinsically modulate dendritic cell maturation to activate T cells and natural killer cells. Hepatology 48:48–58.

French AR, Yokoyama WM. 2003. Natural killer cells and viral infections. Curr Opin Immunol 15:45–51.

Frese M, Schwarzle V, Barth K, Krieger N, Lohmann V, Mihm S, Haller O, Bartenschlager R. 2002. Interferon-gamma inhibits replication of subgenomic and genomic hepatitis C virus RNAs. Hepatology 35:694–703.

Gerlach JT, Diepolder HM, Zachoval R, Gruener NH, Jung MC, Ulsenheimer A, Schraut WW, Schrirren CA, Waechtler M, Backmund M, Pape GR. 2003. Acute hepatitis C: High rate of both spontaneous and treatment-induced viral clearance. Gastroenterology 125:80–88.

Golden-Mason L, Madrigal-Estebas L, McGrath E, Conroy MJ, Ryan EJ, Hegarty JE, O'Farrelly C, Doherty DG. 2008. Altered natural killer cell subset distributions in resolved and persistent hepatitis C virus infection following single source exposure. Gut 57:1121–1128.

Golden-Mason L, Rosen HR. 2006. Natural killer cells: Primary target for hepatitis C virus immune evasion strategies? Liver Transpl 12:363–372.

Irshad M, Khushboo I, Singh S, Singh S. 2008. Hepatitis C virus (HCV): A review of immunological aspects. Int Rev Immunol 27:497–517.

Kashiwakuma T, Hasegawa A, Kajita T, Takata A, Mori H, Ohta Y, Tanaka E, Kiyosawa K, Tanaka T, Tanaka S, Hattori N, Kohara M. 1996. Detection of hepatitis C virus specific core protein in serum of patients by a sensitive fluorescence enzyme immunoassay (FEIA). J Immunol Methods 190:79–89.

Knapp S, Warshow U, Hegazy D, Brackbury L, Guha IN, Fowell A, Little AM, Alexander GJ, Rosenberg WM, Cramp ME, Khakoo SI. 2009. Consistent beneficial effects of killer cell immunoglobulin-like receptor 2DL3 and group 1 human leukocyte antigen-C following exposure to hepatitis C virus. Hepatology 51:1–8.

Lanford RE, Guerra B, Lee H, Averett DR, Pfeiffer B, Chavez D, Notvall L, Bigger C. 2003. Antiviral effect and virus-host interactions in response to alpha interferon, gamma interferon, poly(i)-poly(c), tumor necrosis factor alpha, and ribavirin in hepatitis C virus subgenomic replicons. J Virol 77:1092–1104.

Liu F, Song Y, Liu D. 1999. Hydrodynamics-based transfection in animals by systemic administration of plasmid DNA. Gene Ther 6:1258–1266.

Lohmann V, Korner F, Koch J, Herian U, Theilmann L, Bartenschlager R. 1999. Replication of subgenomic hepatitis C virus RNAs in a hepatoma cell line. Science 285:110–113.

Machida K, Tsukiyama-Kohara K, Seike E, Tone S, Shibasaki F, Shimizu M, Takahashi H, Funata N, Taya C, Yonekawa H, Kohara M. 2001. Inhibition of cytochrome c release in Fas-mediated signaling pathway in transgenic mice induced to express hepatitis C viral proteins. J Biol Chem 276:12140–12146.

Major ME, Mihalik K, Puig M, Rehermann B, Nascimbeni M, Rice CM, Feinstone SM. 2002. Previously infected and recovered chimpanzees exhibit rapid responses that control hepatitis C virus replication upon rechallenge. J Virol 76:6586–6595.

Matsuyama T, Kimura T, Kitagawa M, Pfeffer K, Kawakami T, Watanabe N, Kundig TM, Amakawa R, Kishihara K, Wakeham A. 1993. Targeted disruption of IRF-1 or IRF-2 results in abnormal type I IFN gene induction and aberrant lymphocyte development. Cell 75:83–97.

Minakuchi Y, Takeshita F, Kosaka N, Sasaki H, Yamamoto Y, Kouno M, Honma K, Nagahara S, Hanai K, Sano A, Kato T, Terada M, Ochiya T. 2004. Atelocollagen-mediated synthetic small interfering RNA delivery for effective gene silencing *in vitro* and *in vivo*. Nucleic Acids Res 32:e109.

Ochiya T, Nagahara S, Sano A, Itoh H, Terada M. 2001. Biomaterials for gene delivery: Atelocollagen-mediated controlled release of molecular medicines. Curr Gene Ther 1:31–52.

Ohteki T, Yoshida H, Matsuyama T, Duncan GS, Mak TW, Ohashi PS. 1998. The transcription factor interferon regulatory factor 1 (IRF-1) is important during the maturation of natural killer 1.1+ T cell receptor-alpha/beta+ (NK1+ T) cells, natural killer cells, and intestinal intraepithelial T cells. J Exp Med 187:967–972.

Su AI, Pezacki JP, Wodicka L, Brideau AD, Supekova L, Thimme R, Wieland S, Jens B, Purcell RH, Schultz PG, Chisari FV. 2002. Genomic analysis of the host response to hepatitis C virus infection. Proc Natl Acad Sci USA 99:15669–15674.

Takaku S, Nakagawa Y, Shimizu M, Norose Y, Maruyama I, Wakita T, Takano T, Kohara M, Takahashi H. 2003. Induction of hepatic injury by hepatitis C virus-specific CD8+ murine cytotoxic T